Modulation of Kv3.1b potassium channel level and intracellular potassium concentration in 158N murine oligodendrocytes and BV-2 murine microglial cells treated with 7-ketocholesterol, 24S-hydroxycholesterol or tetracosanoic acid (C24:0)

Maryem Bezine, Sonia Maatoug, Rym Ben Khalifa, Meryam Debbabi, Amira Zarrouk, Yuqin Wang, William J Griffiths, Thomas Nury, Mohammad Samadi, Anne Vejux, et al.

Accepted Manuscript

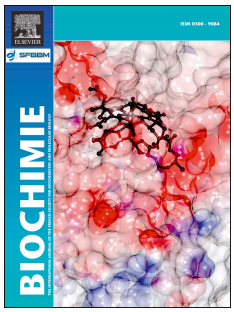

Modulation of Kv3.1b potassium channel level and intracellular potassium concentration in 158N murine oligodendrocytes and BV-2 murine microglial cells treated with 7-ketocholesterol, 24S-hydroxycholesterol or tetracosanoic acid (C24:0)

Maryem Bezine, Sonia Maatoug, Rym Ben Khalifa, Meryam Debbabi, Amira Zarrouk, Yuqin Wang, William J. Griffiths, Thomas Nury, Mohammad Samadi, Anne Vejux, Jérôme de Sèze, Thibault Moreau, Riadh Kharrat, Mohamed El Ayeb, Gérard Lizard

PII: S0300-9084(18)30043-9

DOI: 10.1016/j.biochi.2018.02.008

Reference: BIOCHI 5361

To appear in: *Biochimie*

Received Date: 17 November 2017

Accepted Date: 14 February 2018

Please cite this article as: M. Bezine, S. Maatoug, R. Ben Khalifa, M. Debbabi, A. Zarrouk, Y. Wang, W.J. Griffiths, T. Nury, M. Samadi, A. Vejux, J. de Sèze, T. Moreau, R. Kharrat, M. El Ayeb, G. Lizard, Modulation of Kv3.1b potassium channel level and intracellular potassium concentration in 158N murine oligodendrocytes and BV-2 murine microglial cells treated with 7-ketocholesterol, 24S-hydroxycholesterol or tetracosanoic acid (C24:0), *Biochimie* (2018), doi: 10.1016/j.biochi.2018.02.008.

Modulation of Kv3.1b potassium channel level and intracellular potassium concentration in 158N murine oligodendrocytes and BV-2 murine microglial cells treated with 7-ketocholesterol, 24S-hydroxycholesterol or tetracosanoic acid (C24:0)

Maryem Bezine *et al.*

ABSTRACT

Little is known about K^+ regulation playing major roles in the propagation of nerve impulses, as well as in apoptosis and inflammasome activation involved in neurodegeneration. As increased levels of 7-ketocholesterol (7KC), 24S-hydroxycholesterol (24S-OHC) and tetracosanoic acid (C24:0) have been observed in patients with neurodegenerative diseases, we studied the effect of 24 and/or 48 h of treatment with 7KC, 24S-OHC and C24:0 on Kv3.1b potassium channel level, intracellular K^+ concentration, oxidative stress, mitochondrial dysfunction, and plasma membrane permeability in 158N oligodendrocytes and BV-2 microglial cells. In 158N cells, whereas increased level of Kv3.1b was only observed with 7KC and 24S-OHC but not with C24:0 at 24 h, an intracellular accumulation of K^+ was always detected. In BV-2 cells treated with 7KC, 24S-OHC and C24:0, Kv3.1b level was only increased at 48 h; intracellular K^+ accumulation was found at 24 h with 7KC, 24S-OHC and C24:0, and only with C24:0 at 48 h. Positive correlations between Kv3.1b level and intracellular K^+ concentration were observed in 158N cells in the presence of 7KC and 24S-OHC, and in 7KC-treated BV-2 cells at 48 h. Positive correlations were also found between Kv3.1b or the intracellular K^+ concentration, overproduction of reactive oxygen species, loss of transmembrane mitochondrial potential and increased plasma membrane permeability in 158N and BV-2 cells. Our data support that the lipid environment affects Kv3.1b channel expression and/or functionality, and that the subsequent rupture of K^+ homeostasis is relied with oligodendrocytes and microglial cells damages.

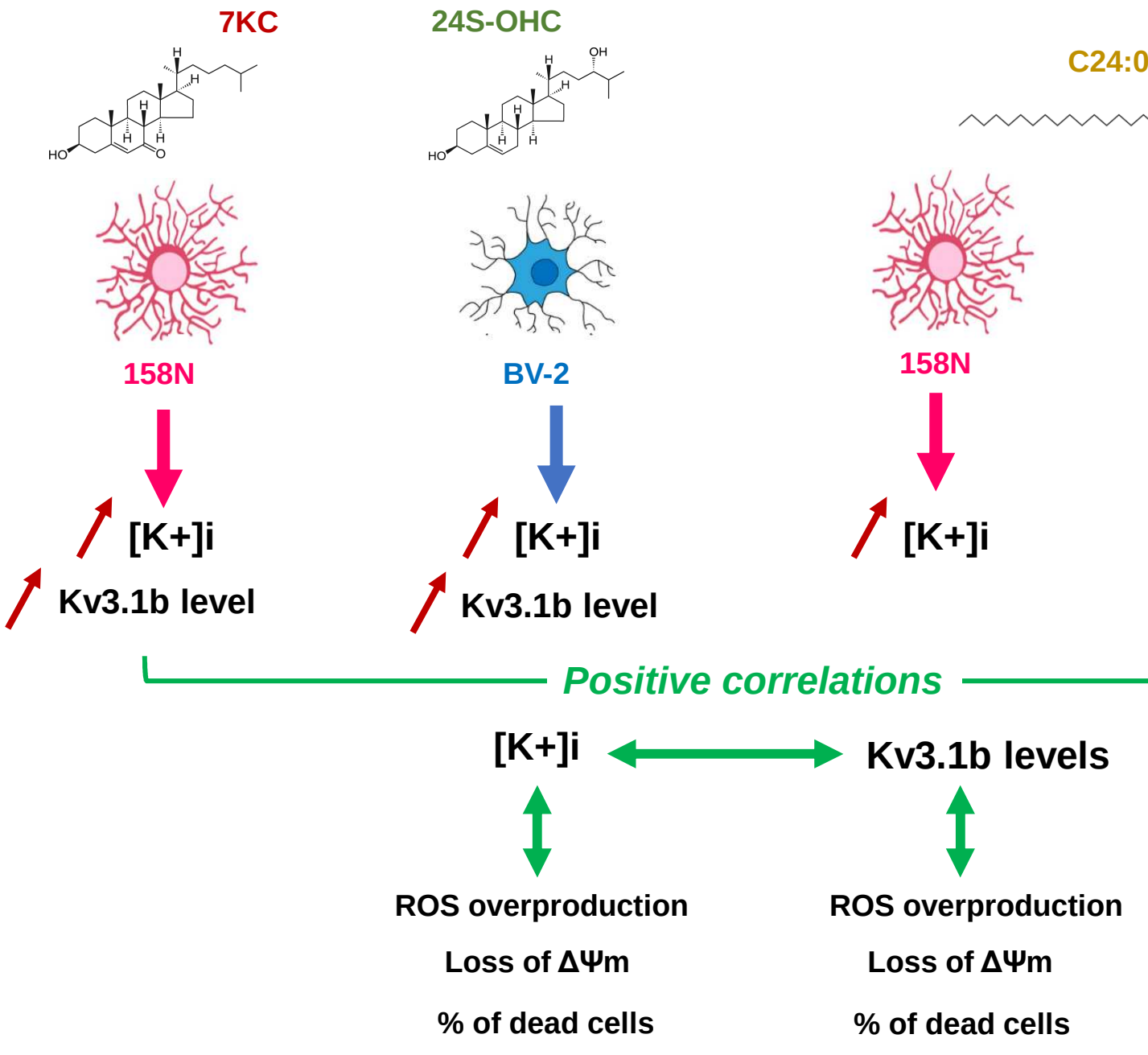

158N murine oligodendrocytes and BV-2 murine microglial cells treated with 7-ketocholesterol, 24S-hydroxycholesterol or tetracosanoic acid (C24:0)

Maryem Bezine [a,b], Sonia Maatoug [b], Rym Ben Khalifa [b], Meryam Debbabi [a,c], Amira Zarrouk [c], Yuqin Wang [d], William J. Griffiths [d], Thomas Nury [a], Mohammad Samadi [e], Anne Vejux [a], Jérôme de Sèze [f], Thibault Moreau [g], Riadh Kharrat [b], Mohamed El Ayeb [b], Gérard Lizard [a]*

[a] Univ. Bourgogne Franche-Comté, Team 'Biochemistry of the peroxisome, inflammation and lipid metabolism' EA 7270 / INSERM, Dijon, France;

[b] Univ. Tunis El Manar – Pasteur Institut, Lab. 'Venoms & Therapeutic Biomolecules', Tunis, Tunisia;

[c] Univ. Monastir, LR12ES05, Lab-NAFS 'Nutrition - Functional Food & Vascular Health', Monastir, Tunisia;

[d] Swansea Univ. Medical School, ILS1 building, Singleton Park, Swansea, UK,

[e] Univ. Lorraine, LCPMC-A2, ICPM, Dept of Chemistry, Metz, France,

[f] Dept. Neurology, Hôpital de Hautepierre, Strasbourg, France.

[g] Dept. Neurology, Univ. Hospital of Dijon, Univ. Bourgogne Franche-Comté / EA7270, Dijon, France

- *Corresponding author (Dr Gérard Lizard) at:*

Univ. Bourgogne Franche-Comté / INSERM, Faculté des Sciences Gabriel
EA7270 / Bio-PeroxIL (Biochemistry of the peroxisome, inflammation and lipid metabolism)
6, Bd Gabriel; 21 000 Dijon, FRANCE
Tel: +33 380 39 62 56 ; Fax: + 33 380 39 62 50 ; E.mail: gerard.lizard@u-bourgogne.fr

Little is known about K^+ regulation playing major roles in the propagation of nerve impulses, as well as in apoptosis and inflammasome activation involved in neurodegeneration. As increased levels of 7-ketocholesterol (7KC), 24S-hydroxycholesterol (24S-OHC) and tetracosanoic acid (C24:0) have been observed in patients with neurodegenerative diseases, we studied the effect of 24 and/or 48 h of treatment with 7KC, 24S-OHC and C24:0 on Kv3.1b potassium channel level, intracellular K^+ concentration, oxidative stress, mitochondrial dysfunction, and plasma membrane permeability in 158N oligodendrocytes and BV-2 microglial cells. In 158N cells, whereas increased level of Kv3.1b was only observed with 7KC and 24S-OHC but not with C24:0 at 24 h, an intracellular accumulation of K^+ was always detected. In BV-2 cells treated with 7KC, 24S-OHC and C24:0, Kv3.1b level was only increased at 48 h; intracellular K^+ accumulation was found at 24 h with 7KC, 24S-OHC and C24:0, and only with C24:0 at 48 h. Positive correlations between Kv3.1b level and intracellular K^+ concentration were observed in 158N cells in the presence of 7KC and 24S-OHC, and in 7KC-treated BV-2 cells at 48 h. Positive correlations were also found between Kv3.1b or the intracellular K^+ concentration, overproduction of reactive oxygen species, loss of transmembrane mitochondrial potential and increased plasma membrane permeability in 158N and BV-2 cells. Our data support that the lipid environment affects Kv3.1b channel expression and/or functionality, and that the subsequent rupture of K^+ homeostasis is relied with oligodendrocytes and microglial cells damages.

KEYWORDS: potassium, Kv3.1b, 7-ketocholesterol, 24S-hydroxycholesterol, oxysterols, tetracosanoic acid (C24:0), 158N cells, BV-2 cells

Abbreviations: 7KC, 7-ketocholesterol; 24S-OHC, 24S-hydroxycholesterol; C24:0, tetracosanoic acid; K^+, Potassium; AD, Alzheimer's disease; MS, Multiple Sclerosis; CSF, cerebrospinal fluid; X-ALD, X-linked adrenoleukodystrophy; VLCFA, very long chain fatty acid; ROS, reactive

$DiOC_6(3)$, 3,3 - dihexyloxacarbocyanine iodide; $O_2^{\bullet-}$, superoxide anion; DHE, dihydroethidium; PI, propidium iodide; $[K^+]_i$, intracellular potassium concentration; MFI, mean fluorescence intensity; ΔΨm, transmembrane mitochondrial potential.

1. INTRODUCTION

Cumulative evidence suggests that the pathophysiogenesis of major neurodegenerative diseases are associated with abnormalities of lipid metabolism, which could favor the rupture of RedOx homeostasis, activation of inflammation, and induction of nerve cell dysfunctions, which are considered hallmarks of neurodegeneration [**1, 2**]. There is evidence that cholesterol and some of its derivatives may contribute to neurodegeneration. The brain is the most cholesterol-rich organ in the body [**3**], about 70% of the cholesterol within the brain is in myelin, the remaining 30% of brain cholesterol is divided between glial cells (20%) and neurons (10%), mainly located in the cellular membrane [**4**]. In humans, the causal relationship between cholesterol and dementia needs to be clarified [**5**]. However, this does not exclude the possibility that cholesterol transport and metabolism probably play key roles in the development of Alzheimer's disease (AD). Indeed, the strongest genetic risk factor for AD is *APOE*-ε4 [**6**]. Since oxysterols, which are oxygen derivatives of cholesterol (formed enzymatically and/or by auto-oxidation) [**7**], are thought to reflect cerebral cholesterol turnover, there has been great interest in the diagnostic and prognostic value of these metabolites in neurodegenerative diseases [**8**]. The key role of oxysterols in AD has been strongly supported by research pointing to their involvement in modulating neuroinflammation, Aβ accumulation, and cell death [**9**]. One cholesterol oxide derivative, 24(S)-hydroxycholesterol (24S-OHC; also named cerebrosterol) could constitute a potential biomarker of neurodegeneration, especially of AD [**10**]. 24S-OHC is synthesized in the brain via CYP46A1

memory [**12**]. Either decreased or increased concentrations of 24S-OHC were found in the plasma and cerebrospinal fluid (CSF) of patients with AD. Decreased 24S-OHC concentrations in the plasma of AD patients were attributed to brain atrophy, which could be a consequence of the decrease in metabolically active neurons [**13**]. On the other hand, a significant increase in 24S-OHC, correlating with an increase in the tau protein level, has been described in the CSF of patients with mild cognitive impairment (MCI) and AD [**14, 15**]. Higher plasma and CSF levels of 24S-OHC have also been reported in AD patients and in patients with vascular dementia **[16, 17]**. These data favor the hypothesis that 24S-OHC may be a good marker of "brain health" in old age, and would be increased during the progression of AD and decrease in later stages. As elevated concentrations of 24S-OHC induce cell death in neuronal cells [**18, 19]**, it has been suggested that 24S-OHC-induced lipotoxicity might contribute to neurodegeneration and brain atrophy. Among oxysterols, a variety of compounds that are derived from cholesterol autoxidation were also identified at increased levels in the frontal and occipital cortex. These included 7-ketocholesterol (7KC; also named 7-oxocholesterol), 7α-hydroxycholesterol, 4β-hydroxycholesterol, 5α, 6α-epoxycholesterol, and 5β, 6β-epoxycholesterol [**20**]. Increased levels of 7KC were also identified in the plasma and/or CSF of patients with major neurodegenerative diseases such as multiple sclerosis (MS) [**21, 22**]**,** X-linked adrenoleukodystrophy (X-ALD) [**23**], and Niemann-Pick disease [**24, 25**]. As 7KC is a potent inducer of oxidative stress, inflammation and cell death, which are major events associated with major ageing-related diseases, including AD [**26**], its contribution to neurodegeneration is widely suspected. In addition, 7KC has been shown to trigger not only mitochondrial but also peroxisomal dysfunctions leading to increased levels of very long chain fatty acids (VLCFA; C≥22), which could favor brain damages [**27**]. Thus, in peroxisomal leukodystrophies, resulting from either peroxisome biogenesis disorders or

C26:0, are observed in the plasma and tissues of patients [**28**]. In the cortical region of patients with AD at the stage V–VI of the disease, an accumulation of C22:0 as well as of C24:0 and C26:0, which are substrates for peroxisomal β-oxidation [**29**], have been found [**30**]. In addition, the level of plasmalogens (etherphospholipids), which need intact peroxisomes for their biosynthesis [**31, 32]**, was decreased in severely affected tissues [**30**] supporting peroxisomal dysfunctions [**33**]. In the erythrocytes and plasma of patients with AD, increased levels of C26:0 were also observed, thus suggesting that peroxisomal dysfunctions and/or alterations of desaturase and elongase activities may contribute to cognitive dysfunctions [**34, 35**]. Moreover, increased levels of VLCFA have also been described in the relapsing remitting and secondary progressive forms of MS [**36**].

At the moment, several data indicate that 7KC, 24S-OHC and C24:0 are potent inducers of neurodegeneration, mainly via their ability to promote overproduction of reactive oxygen species (ROS) and mitochondrial dysfunctions [**20, 25, 37**], which could subsequently contribute to inflammation and cell death [**27, 38**]. However, little is known about their ability to disturb ionic homeostasis, which is involved in major biological processes necessary for the proper functioning of the central and peripheral nervous system, such as signal transmission and the propagation of nerve impulse. Depending on the cell type considered, 7KC and 24S-OHC are able to modulate or not intracellular Ca^{2+} level [**39, 40, 41**], and in human retinal cells, 7KC-induced toxicity has been reported to activate the P2X7 receptor which leads to Na^{+} and Ca^{2+} influx, and K^{+} efflux [**42**]. Activation of P2X7 receptor triggers the formation of large nonselective membranes pores which results in inflammation through the inflammasome, oxidative stress and, ultimately, cell death especially by apoptosis [**42**]. In mitochondria of wild-type and *Abcd1*$^{-/-}$ mice, it was also described that C24:0-induced cytotoxicity diminished the mitochondrial Ca^{2+} retention capacity

from rat hippocampus culture [**44**]. These different effects suggest that C24:0-induced cytotoxicity could be due to its dramatic effects on mitochondrial dysfunction and Ca^{2+} deregulation. However, nothing is known about the impact of C24:0 on K^+ homeostasis. Additionally, in bone marrow derived-macrophages from *Abcd1*$^{+/-}$ C57BL/6 mice, glibenclamide (a K^+ efflux inhibitor) was able to block inflammasome activation and IL-1β secretion, which is thought to contribute to demyelination and brain degeneration in patients with X-linked adrenoleukodystrophy (X-ALD) [**45**]. ATP-sensitive potassium (KATP) channels localized in the plasma membrane and in the inner mitochondrial membrane have been shown to play important roles in modulating neuronal excitability, cell survival, and cerebral vascular tone. Interestingly, diazoxide, which is a KATP activator, can ameliorate molecular, cytopathological, and behavioral alterations in 3xTg mice, which constitute a mouse model of AD [**46**]. As sustained-release fampridine, a slow release formulation of 4-aminopiridine (4-AP), is used for the treatment of walking difficulties in MS, and is considered efficient for the symptomatic management of this disease [**47**], it can be supposed that better understanding of the regulation of K^+ homeostasis in MS patients, and in patients with AD, where a potential role of K^+ is suspected [**48**], might lead to the identification of new therapeutic targets and new treatments. It has thus been thought that voltage-gated K^+ (Kv) channels, mainly Kv3.1 designed for high-frequency repetitive firing and expressed by different types of nerve cells in the CNS [**49, 50**], could constitute new therapeutic targets [**51**]. This hypothesis is reinforced by the following observations: in the neocortex of aged APPPS1 mice (a transgenic model of Alzheimer's disease), Kv3.1 mRNA and protein levels were significantly lower compared to wild type, suggesting that a decrease in Kv3 currents could play a role in the cognitive symptoms of AD [**52]**; 4-AP modulation of an Aβ(1-42)-induced I(K) (candidate channel Kv3.1) in human microglia could

splicing of the Kv3.1 gene gives rise to two isoforms that differ only in their COOH-terminal sequence, the last 18 amino acid sequences in Kv3.1a are replaced by 84 amino acid residues in Kv3.1b [**54, 55, 56**]. Interestingly, in the mature nervous system, the Kv3.1b splice variant of this channel predominates [**57**].

As demyelinating and non-demyelinating neurodegenerative diseases involve microglial activation, which could have detrimental and beneficial effects depending on the stage of the diseases [**58**], it was of important to determine the impact of 7KC, 24S-OHC and C24:0 on BV-2 murine microglial cells. In addition, as a deterioration of the white matter does not seem specific to neurodegenerative demyelinating diseases, such as MS and peroxisomal leukodystrophies, and has been reported in patients with dementia [**59**], it was of interest to determine the impact of 7KC, 24S-OHC and C24:0 on oligodendrocytes, which are myelin synthetizing cells in the central nervous system [**60**]. Indeed, there is now evidence that the breakdown of myelin is associated with AD. It is supposed that the vulnerability of oligodendrocytes in AD induces myelin breakdown and the loss of the myelin sheath, which might be the initiating step of the changes in the earliest stage of AD, prior to appearance of amyloid and tau pathology [**61**]. To this end, 158N murine oligodendrocytes and BV-2 murine microglial cells were cultured without or with 7KC, 24S-OHC and C24:0, and the effects of these lipids on Kv3.1b level, intracellular K^+concentration, ROS overproduction, mitochondrial activity, and plasma membrane integrity were determined.

2. MATERIALS AND METHODS

2.1. Cells, cell cultures and treatments

Tabby male (Ta/Y) control mice [**62**], show several characteristics of differentiated oligodendrocytes [**63**]. 158N cells were plated at a density of 34 x 10^3 cells / cm^2 in Dulbecco's modified Eagle medium with L-glutamine (Lonza, Levallois, France) supplemented with 5% heat-inactivated fetal bovine serum (FBS) (Pan Biotech, Aidenbach, Germany) and 1% antibiotics (100 U/mL penicillin, 100 mg/mL streptomycin) (Pan Biotech).

Murine microglial cells (BV-2) were from Banca-Biologica Cell Factory (IST Genoa, Italy). They were seeded at a density of 17 x 10^3 cells / cm^2 in RPMI 1640 (Lonza, Amboise, France) supplemented with 10% (*v*/*v*) heat-inactivated fetal bovine serum (FBS) (Pan Biotech, Aidenbach, Germany) and 1% antibiotics (100 U/mL penicillin, 100 mg/mL streptomycin) (Pan Biotech).

158N and BV-2 cells were incubated at 37 °C in a 5% CO_2 humidified atmosphere in tissue culture dishes (100 × 20 mm, FALCON, Corning, Tewksbury, MA, USA) (with 10 mL of culture medium), or per 12-wells plate (with 1 mL of culture medium). After 24 h of culture, cells were treated for 24 h with either oxysterols (7KC or 24S-OHC), or C24:0 used in a range of concentrations from 2.5 to 25 µM, and from 1 to 20 µM, respectively. Initial solutions of 7-ketocholesterol (7KC) (Ref: C2394, Sigma-Aldrich, St Quentin Fallavier, France) and 24S-hydroxycholesterol (24S-OHC) (provided by Prof. M. Samadi, Univ. Lorraine, Metz, France) were prepared as previously described to obtain a final concentration of 2 mM [**64, 65**]. Briefly, to prepare the initial solution, 800 µg of oxysterols (7KC or 24S-OHC) were dissolved in 50 µL of absolute ethanol (EtOH), used as vehicle, and 950 µL of culture medium was added. Tetracosanoic acid (C24:0) (Sigma-Aldrich) was prepared at 400 µM in α-cyclodextrin (vehicle) (Sigma-Aldrich). The maximal final concentration of absolute ethanol or α-cyclodextrin in the culture medium was 0.05% and 1 µM, respectively [**41, 65, 66, 67**]. The concentrations of 7KC,

with 7KC and 24S-OHC, and 158N and SK-N-BE cells treated with C24:0 [**19, 41, 65, 66, 67]**. In the heat inactivated FBS used the concentration of C24:0 was very low (682.20 nmol/L), and no 7KC and 24S-OHC were detected [**68**]. 4-aminopyridine (4-AP: 4 mM) (Sigma-Aldrich) was prepared as a stock solution at 800 mM and 200 mM in culture medium, respectively. 4-AP was incubated with the cells for 1h prior to incubation with 7KC, 24S-OHC and C24:0.

2.2. Measurement of transmembrane mitochondrial potential with $DiOC_6$(3)

Variations in the mitochondrial transmembrane potential (ΔΨm) were measured with the cationic lipophilic dye 3,3′- dihexyloxacarbocyanine iodide ($DiOC_6$(3) (Life Technologies / Thermo Fisher Scientific, Courtaboeuf, France). Cells treated or not with 7KC, 24S-OHC (2.5 to 25 μM) or C24:0 (1 to 20 μM) for 24 h were pooled, and stained for 10 min at 37°C with $DiOC_6$(3) used at 40 nM; mitochondrial depolarization (loss of ΔΨm) is indicated by a decrease in green fluorescence measured by flow cytometry. Green fluorescence was collected through a 520 ± 10 nm bandpass filter on a Galaxy flow cytometer (Partec, Münster, Germany). A total of 10,000 cells were analyzed for each sample, and the fluorescent signals were measured on a logarithmic scale. Data were analyzed with Flomax (Partec) or FlowJo (Tree Star Inc., Ashland, OR, USA) software.

2.3. Measurement of reactive oxygen species production with dihydroethydium

Overproduction of superoxide anion ($O_2^{\bullet -}$) were detected with dihydroethidium (DHE; Life Technologies) [**69**]. DHE, a non-fluorescent compound, diffuses through cell membranes and is rapidly oxidized in ethidium under the action of reactive oxygen species, mainly $O_2^{\bullet -}$ [**69**]. Control (untreated cells), 7KC, 24S-OHC (2.5 to 25 μM) or C24:0 (1 to 20 μM) -treated cells

DHE-stained cells were collected through a 520/20 nm bandpass filter. Fluorescent signals were measured on a logarithmic scale on a GALAXY flow cytometer (Partec); 10,000 cells were acquired; data were analyzed with Flomax (Partec) or FlowJo (Tree Star Inc.) software. Three independent experiments carried out in triplicate were performed.

2.4. Quantification of cell death by staining with propidium iodide

Control (untreated cells), 7KC, 24S-OHC (2.5 to 25 μM) or C24:0 (1 to 20 μM) -treated cells were pooled and stained for 10 min with propidium iodide (PI: 1 μg/mL), a fluorescent compound which enters dead cells or cells with damaged cytoplasmic membranes [**70**]. Membrane permeability was analyzed with a Galaxy flow cytometer (Partec) equipped with a 488-nm blue laser. Red fluorescence of PI was collected on a logarithmic scale of fluorescence using a 590 ± 10 nm bandpass filter and analyzed with Flomax (Partec) or FlowJo (Tree Star Inc.) software.

2.5. Measurement of intracellular potassium by flame photometry

Intracellular potassium $[K^+]_i$ was measured using a Flame Photometer (Biocode Hycel PHF 108, Biocode Hycel, Liège, Belgium) with a propane flame; lithium was used as an internal standard. After 24 h of culture, cells were treated for 24 h with either oxysterols (7KC, 24S-OHC (2.5 to 25 Mm)) or C24:0 (1 to 20 μM). Cells were washed with HBSS (pH=7.4), resuspended in 1 mL of deionized water and lysed by repeated cycles of freezing and thawing. They were then centrifuged at 3000 rpm for 10 min. The supernatant was analyzed.

microscopy

Kv channels are pore-forming subunits of voltage-dependent potassium channels which can be detected with the use of different antibodies [**71**]. Identification and quantification of Kv3.1 were performed on cell suspensions and deposits by flow cytometry and fluorescence microscopy, respectively. Cells were collected, washed in PBS, 1% BSA, 0.1% NaN_3, resuspended in PBS, and fixed in freshly prepared 2% (w/v) p-formaldehyde diluted in PBS (pH 7.4) (10 min; room temperature). Cells were permeabilized with (PBS, 0.05% saponin (Sigma–Aldrich), 10% FBS (Pan Biotech)) for 20 min. After two washes in PBS, cells were incubated (1 h; 4°C) with the primary antibody directed against Kv3.1 diluted at 1:100 in the permeabilizing buffer (rabbit polyclonal (Abcam, Cambridge, UK); ref: ab101693, mouse monoclonal (Santa-Cruz Biotechnology, Santa-Cruz, CA, USA); ref: sc-514554; mouse monoclonal (Sigma-Aldrich); ref: SAB5200030 (anti-kv3.1b)). Cells were then washed twice with PBS and incubated (1 h; room temperature) with a 488-Alexa goat anti-rabbit (Abcam) or a goat anti-mouse (Invitrogen / Thermo Fisher Scientific) used at 1/500. A conjugated control (without primary antibody) was performed. Cells were washed and resuspended in PBS, and analyzed by flow cytometry on a Galaxy flow cytometer (Partec). The green fluorescence of 488-Alexa was collected with a 520/10 nm bandpass filter. For each sample, 10,000 cells were acquired, and the data were analyzed with Flomax (Partec) or FlowJo (FlowJo Inc.) software. For fluorescence microscopy analyses, nuclei were counterstained with Hoechst 33342 (Sigma–Aldrich) used at a concentration of 2 µg/mL. After washing with PBS, cell deposits were obtained by cytocentrifugation with a cytospin 4 centrifuge (Shandon, Cheshire, UK). Slides were mounted and observed with an Axioskop Zeiss microscope, and digitalized images were obtained with an Axiocam Zeiss camera (Zeiss, Jena, Germany).

2.7. Polyacrylamide gel electrophoresis and western blotting

Cells washed in PBS were lysed in 100 µL of cold radio-immunoprecipitation assay buffer (RIPA) (10 mM Tris–HCl, pH 7.2, 150 mM NaCl, 0.5% Nonidet NP40, 0.5% Na deoxycholate, 0.1% SDS, 2 mM EDTA and 50 mM NaF) containing 1:25 protease inhibitor cocktail (Roche Diagnostics Corporation, Meylan, France). After incubation on ice for 30 min, samples were centrifuged at 14,000×g in an Eppendorf microcentrifuge for 15 min at 4°C, and the supernatant was recovered. The protein concentration was measured in the supernatant using the Bicinchoninic Acid Assay (Sigma-Aldrich). Seventy micrograms of protein were resolved in gel loading buffer (125 mM Tris-HCl, pH 6.8, 4.6% SDS, 20% glycerol, 0.003% bromophenol blue) and separated on a 10% sodium dodecyl sulfate–polyacrylamide gel then subsequently transferred onto nitrocellulose membranes (Thermo Fisher Scientific). After blocking for 1 h with 5% BSA in PBST (0.1% Tween 20) (Sigma-Aldrich), membranes were incubated overnight at 4°C with the primary antibody raised against Kv3.1b (1:500 (mouse monoclonal; ref: SAB5200030; Sigma-Aldrich)) diluted with PBST, 1% BSA. Antibody directed against β-actin (1:5000 (mouse monoclonal antibody; ref: A2228; Sigma-Aldrich)) was used to detect reference protein expression. The membrane was then washed twice with PBST and incubated for 1 h at room temperature with horseradish peroxidase-conjugated goat anti-mouse antibody (Cell Signaling Technology, Danvers, MA, USA) diluted at 1:5,000. Immunopositive bands were visualized by the enhanced chemiluminescence kit (Super Signal West Femto Maximum Sensitivity Substrate, Thermo Fisher Scientific) and Chemidoc XRS^{+} (Santa Cruz Biotechnology). Semi-quantification of Kv3.1b luminescence signal intensity versus actin was determined by computer-assisted analyses of optical density using Image Lab 4.0.1 software (Bio-Rad, Marnes La Coquette, France).

Fifty µL of PBS was added to the cell pellet (about 1 x 10^7 cells) followed by 1.05 mL absolute ethanol while under sonication. Sonication was continued for a further 5 min. After a brief vortex, the suspension was transferred to a microcentrifuge tube and centrifuged at 16,000 g at 4°C for 30 min. The supernatant was diluted to 70% ethanol by the addition of 0.4 mL of water. Oxysterols were separated from cholesterol and other sterols of similar polarity in the resulting solution by solid phase extraction (SPE) on a Waters Sep-Pak tC18 column (200 mg) essentially as described in Abdel-Khalik *et al.* [**72**]. In brief, after washing the SPE column with absolute ethanol (4 mL) followed by 70% ethanol (6 mL), the cell extract (1.5 mL, 70% ethanol) was added to the column followed by a wash of 5.5 mL 70% ethanol. Oxysterols elute in the flow-through and column-wash (7 mL 70% ethanol), while cholesterol remains on the column. The oxysterol fraction was divided into two equal sub-fractions (A) and (B) and lyophilised.

2.9. Oxysterol derivatisation

The derivatisation procedure was essentially as described in Abdel-Khalik *et al.* [**72**]. In brief, each sub-fraction (A) and (B) was reconstituted in propan-2-ol (100 µL). Sub-fraction (A) was incubated with 1 mL of phosphate buffer (50 mM, pH 7) containing cholesterol oxidase (0.26 u) from Streptomyces sp (Sigma Aldrich) for 1h at 37°C. The reaction was quenched with methanol (2 mL). Sub-fraction (B) was treated in an identical fashion but in the absence of cholesterol oxidase.

Glacial acetic acid (150 µL) was added to both sub-fractions which were derivatised with the Girard P (GP) reagent; (A) with [2H5]GP (190 mg, bromide salt) [**73**] and (B) with [2H0]GP (150 mg, chloride salt, TCI Europe) at room temperature, overnight in the dark.

washing the column with methanol (6 mL), 10% methanol (6 mL) and 70% methanol (4 mL), the derivatisation mixture (3.25 mL, 70% organic) was loaded on the column followed by a wash with 70% methanol (1 mL) and 35% methanol (1 mL). The flow-through and washes were collected and diluted with water to give 35% methanol (9 mL). This was re-cycled through the column and the dilution procedure repeated to give 17.5% methanol (19 mL) which was re-cycled through the column once again. The effluent was discarded. The column was then washed with 10% methanol (6 mL). At this point all oxysterols are bound to the column while derivatisation reagent has been removed. Finally, oxysterols were eluted with methanol (2 mL).

2.10. LC-MS(MSn) analysis

Sub-fraction (A) contains oxysterols derivatised with [2H5]GP at position C-3 after treatment with cholesterol oxidase. Sub-fraction (B) contains oxysterols derivatised with [2H0]GP at position C-7 in the absence of cholesterol oxidase. Prior to LC-MS(MS)n analysis equal aliquots of sub-fractions (A) and (B) were combined and diluted to 60% methanol. Analysis was performed on an LTQ-Orbitrap Elite (Thermo Fisher Scientific) equipped with an electrospray probe and an Ultimate 3000 LC system (Dionex, now Thermo Fisher Scientific) as previously described [**73**]. For each injection four scan events were performed (one high resolution scan 120,000 at m/z 400) and four multistage fragmentation events in the LTQ linear ion trap.

2.11. Statistical analysis

Statistical analyses were carried out with GraphPad Prism 6.07 software. Data were expressed as mean ± SEM and statistical analyses were performed by two-way ANOVA (Tukey's test). The

values < 0.05 were considered statistically significant.

3. RESULTS

3.1. Evaluation of the expression of Kv3.1 protein in 158N murine oligodendrocytes and BV-2 murine microglial cells

The presence of Kv3.1 protein (Kv3.1a and/or Kv3.1b) in 158N and BV-2 cells was detected by flow cytometry (**Fig. 1A**) and immunofluorescence microscopy (**Fig. 1B**). The levels of Kv3.1 protein were studied using either a mouse monoclonal antibody raised against amino acids 118-179 (Santa Cruz antibody recognizing Kv3.1a and Kv3.1b), a rabbit polyclonal antibody (Abcam from unknown specificity regarding the a and b subtype of Kv3.1), and a mouse monoclonal antibody raised against a peptide corresponding to the C terminus (437-585) (Sigma-Aldrich antibody recognizing Kv3.1b). With all antibodies used, strong expression of Kv3.1 was observed in both 158N and BV-2 cells: the percentage of Kv3.1 positive cells ranged from 90 to 98%, and the mean fluorescence intensity (MFI) was always stronger than that in conjugated controls (**Fig. 1A**). This high expression of kv3.1 was confirmed by fluorescence microscopy (**Fig. 1B**). Altogether, our data indicate that Kv3.1 is strongly expressed by 158N and BV-2 cells. Further analyses were conducted by western blotting in order to determine the specificity of the antibodies used. In our hands, the Santa-Cruz antibody was not suitable to perform western blot analyses. As the specificity of the Abcam antibody was not provided by the manufacturer, immunoblot analysis was not done. It is noteworthy that immunoblot analysis of total protein extracts performed with the Sigma-Aldrich antibody revealed a single band at around 66 kDa corresponding to the core Kv3.1b [**71**] **(Fig. 1C)**. For further analyses, the Sigma-Aldrich

expression.

3.2. Effect of 7-ketocholesterol, 24S-hydroxycholesterol and tetracosanoic acid (C24:0) on Kv3.1b channel level in 158N and BV-2 cells

Flow cytometric analyses associated or not with western blotting were performed to investigate the effects of 7KC, 24S-OHC and C24:0 on Kv3.1b level in158N and BV-2 cells. To this end, 158N cells were cultured for 24 h without (control), or with 7KC (2.5 to 25 µM), 24S-OHC (2.5 to 25 µM) and C24:0 (1 to 20 µM), or with the different vehicle (EtOH (0.005 to 0.05%); α-cyclodextrin (0.05 to 1 mM)). After 24 h of treatment with 7KC (25 µM, 24h) and 24S-OHC (25 µM, 24h), no 7KC and 24S-OHC metabolites listed in **Supplementary Fig. 1A-B** were detected in 158N and BV2-treated cells as well as in control cells and vehicle-treated cells. The level of Kv3.1b was simultaneously analyzed by flow cytometry and western blotting. Under treatment with 7KC and 24S-OHC, flow cytometric analyses showed an increase in Kv3.1b level at 12.5 and 25 µM as compared with the corresponding EtOH-treated cells (**Fig. 2A**). No significant difference was observed between untreated cells (control) and EtOH-treated cells at 0.005% and 0.025% (**Fig. 2A**). These data are in agreement with those obtained by western blot analysis, which also revealed a significant increase in Kv3.1b under treatment with 7KC (2.5 µM) (**Fig. 2B**). With C24:0, used in a range of concentration from 1 to 20 µM, no modification of Kv3.1b level was found by either flow cytometry or western blot analysis; no difference was observed between control and α-cyclodextrin-treated cells (**Fig. 2A and B**).

In BV-2 cells, by flow cytometry, no significant modulation of Kv3.1b level was revealed after 24 h of treatment with oxysterols (7KC or 24S-OHC: 2.5 to 25 µM) or C24:0 (1 to 20 µM) (**Fig.**

and 24S-OHC (25 µM) and with C24:0 (10 µM) (**Fig. 3B**).

3.3. Effects of 7-ketocholesterol, 24S-hydroxycholesterol and tetracosanoic acid (C24:0) on the intracellular K^+ level

The impact of 7KC (2.5 to 25 µM), 24S-OHC (2.5 to 25 µM) and C24:0 (1 to 20 µM) on $[K^+]i$ was determined in 158N and BV-2 cells by flame photometry (**Fig. 4)**. 4-AP (4 mM), a universal Kv channel blocker, was used as a positive control to favor K^+ accumulation.

In 158N cells, marked effects of 7KC and 24S-OHC were detected on $[K^+]i$. Significant increases in $[K^+]i$ were induced by 7KC and 24S-OHC from 2.5 to 25 µM as compared with the corresponding vehicle (EtOH) concentration (**Fig. 4 A)**. Lower K^+ accumulation was observed with C24:0, even though significant increases were detected from 5 to 20 µM (**Fig. 4A)**. With the vehicles, as compared with untreated cells, slight effects were detected with EtOH at 0.05% only (**Fig. 4A**).

The result obtained for BV-2 cells, after 24 h with either 7KC, 24S-OHC or C24:0 showed a slight effect on $[K^+]i$ (**Fig. 4B**). After 48 h of treatment with 7KC or 24S-OHC, as compared with the corresponding vehicle (EtOH), no significant differences were observed (**Fig. 4C**). After 48 h of treatment with C24:0, a slight but significant increase was observed at 20 µM only (**Fig. 4C**). No difference was observed between control and vehicle (EtOH or α-cyclodextrin) (**Fig. 4B and C**).

3.4 Evaluation of the correlation between Kv3.1b level and intracellular potassium concentration

7KC for 24 h ($r = 0.83$; $p < 0.0001$) and in BV-2 cells treated for 24 h ($r = 0.65$; $p=0.056$) and 48 h ($r = 0.68$; $p < 0.013$) (**Fig. 5)**. With 24S-OHC a significant correlation was observed in 158N only ($r = 0.74$; $p = 0.0009$) (**Fig. 5)**. No correlation was observed under treatment with C24:0 (**Fig. 5**).

3.5. Evaluation of the correlation between Kv3.1b level, intracellular potassium, and cell damages

The correlation between Kv3.1b level, $[K^+]i$ and cell damages induction was studied by taking into account the percentage of $DiOC_6(3)$-negative cells, and DHE- and PI-positive cells (**Tables 1 and 2**). The percentage of $DiOC_6(3)$-negative cells (cells with depolarized mitochondria), of DHE-positive cells (cells which overproduce $O_2^{\bullet -}$) and PI-positive cells (cells with damaged plasma membrane and/or dead cells) among 158N cells treated for 24 h with 7KC (2.5 to 25 µM), 24S-OHC (2.5 to 25 µM), and C24:0 (1 to 20 µM) are shown in **Supplementary Table 1**. The percentage of $DiOC_6(3)$-negative cells, and of DHE- and PI-positive cells among BV-2 cells treated with 7KC (2.5 to 25 µM), 24S-OHC (2.5 to 25 µM), and C24:0 (1 to 20 µM) for 24 and 48 h are shown in **Supplementary Tables 2 and 3**, respectively.

In agreement with previous report [**63-66**], 158N cells treated with 7KC, 24S-OHC, and C24:0 for 24 h, showed a loss of transmembrane mitochondrial potential ($\Delta\Psi m$), revealed by an increase in the percentage of $DiOC_6(3)$-negative cells (**Supplementary Table 1**). This was associated with the overproduction of $O_2^{\bullet -}$, revealed by increased percentages of DHE-positive cells, and with damaged plasma membranes and/or cell death induction, indicated by increased percentages of PI-positive cells (**Supplementary Table 1**).

slight increases in $DiOC_6(3)$-negative cells, DHE-positive cells, and PI-positive cells were observed (**Supplementary Table 2**). At 48 h, marked effects of 7KC were mainly found (**Supplementary Table 3**).

In 158N cells (24 h), the analysis of the correlation between the Kv3.1b level (MFI measured by flow cytometry) and $DiOC_6(3)$-negative cells, DHE- and PI-positive cells, showed a marked positive correlation in cells treated with 7KC and 24S-OHC, and no significant correlation with C24:0-treated cells (**Table 1 and supplementary Fig. 2**). A significant positive correlation was observed between the Kv3.1b level and $DiOC_6(3)$-negative cells for BV-2 cells treated for 24 hours with 7KC and C24:0, and between the Kv3.1b level and $DiOC_6(3)$-negative cells, DHE-positive cells, and PI-positive in BV-2 cells treated with 24S-OHC (**Table 1 and supplementary Fig. 3**). A significant positive correlation was also observed between the Kv3.1b level and $DiOC_6(3)$-negative cells, DHE-positive cells, and PI-positive cells in BV-2 cells treated with 7KC and 24S-OHC for 48 h whereas no correlations were found with C24:0 (**Table 1 and supplementary Fig. 4**).

For 158N and BV-2 cells (24 h), the analysis of the correlation between $[K^+]i$ (measured by flame photometry) and $DiOC_6(3)$-negative cells, DHE- and PI-positive cells showed significant positive correlations (**Table 2 and supplementary Fig. 5 and 6**). In BV-2 cells (48 h), 7KC and C24:0 were associated with significant positive correlations between $[K^+]i$, $DiOC_6(3)$-negative cells, DHE- and PI-positive cells; no correlations were found with 24S-OHC (**Table 2 and supplementary Fig. 7).**

Increased levels of 7KC, 24S-OHC and/or C24:0 have been reported in major neurodegenerative diseases: AD [**17, 25, 20, 74**, **75**], MS [**22, 76, 77, 78**]**,** Parkinson's disease [**79**], X-ALD [**23]**, Huntington's disease [**80, 81**], and Niemann-Pick disease [**24, 25**, **82**]. It is therefore suspected that 7KC, 24S-OHC and C24:0, which are known to induce important cell dysfunctions including oxidative stress on nerve cells in vitro [**65, 66**], could contribute to favor neurodegeneration. As it has been reported that modulation of K^+ channel activities by oxidative stress can constitute a significant determinant in aging and neurodegenerative diseases [**83 - 88**], and as modifications of [K+]i can contribute to inflammation [**88**] and to cell death induction [**68, 89**], which are hallmark of brain degeneration, the impact of 7KC, 24S-OHC and C24:0 was simultaneously studied on Kv3.1b channel level and $[K^+]$i on oligodendrocytes and microglial cells involved in neurodegenerative diseases [**90, 91]**. Altogether, our data obtained on 158N murine oligodendrocytes and on murine microglial BV-2 cells confirm that the lipotoxicity of 7KC, 24S-OHC and C24:0 favors a rupture of K^+ homeostasia leading to increased $[K^+]$i [**68**], and they establish that intracellular K^+ accumulation is associated with more or less pronounced modulations of Kv3.1b level.

In the present study, we described for the first time, the presence of Kv3.1b protein in both 158N and BV-2 cells. It is known that Kv3.1b channel expression is widespread in the nervous system; in adult brain, Kv3.1b mRNA is far more abundant than the Kv3.1a transcript, with both transcripts strongly expressed in neuronal subpopulations of the olfactory bulb, neocortex, hippocampus, basal nuclei, thalamus, brainstem, and cerebellum [**56**, **92**]. Our attention focused on Kv3.1b channel because it was identified that Kv3.1 is expressed in significant quantities in oligodendrocyte cells and plays important role in their structure and function [**93**]. Notably, a reduction in myelin thickness and a decrease in the number of large-diameter axons was observed

is up-regulated in microglia activation and could regulate the production of pro-inflammatory signaling molecules such as IL-1β, IL-6, TNFα and nitric oxide [**53, 94]**. A rapid modulation of the expression of Kv3.1 channel has also been detected in $A\beta_{1-42}$-treated microglia [**53**].

Our study also shows that 7KC, 24S-OHC and C24:0 induce ROS overproduction and cell damages (loss of transmembrane mitochondrial potential, increased permeability of plasma membrane) on 158N murine oligodendrocytes and BV-2 microglial cells. However, the possible interaction of these compounds with Kv channels remained obscure, especially the impact of voltage-gated K^+ (Kv) on cell damages. As 7KC is known to modify membrane fluidity [**95 - 97]**, and as several membrane properties are modified by oxysterols, which are oxidized either on the steroid nucleus or on the side chain [**97]**, we can suppose that 7KC and 24S-OHC can execute important functions via interactions with plasma membrane components including Kv3.1 channel and P2X7 receptor, leading to modifications of their activities. In the presence of C24:0, which could modify the phospholipid composition and consequently plasma membrane properties (as reported for other fatty acids) [**98**], we can also suppose an effect of C24:0 on the biophysical membrane characteristics which could further impact the properties of several membrane components. The present data underline that the most important up-regulation of Kv3.1b occurs on 158N cells under treatment with 7KC and 24S-OHC, and are less important mainly on BV-2 cells treated with 7KC. We found an dose-dependent increased of Kv3.1b level along with increasing percentage of damaged cells revealed by higher percentages of $DiOC_6(3)$ negative cells (cells with depolarized mitochondria), DHE positive cells (cells overproducing $O_2^{\bullet -}$) and PI positive cells (cells with damaged plasma membrane and/or dead cells), indicating that K3.1b is associates to cell damages involved in cell death induction. These data underline that the modulation of Kv3.1b level depends on the type of nerve considered. To better explore this

level was associated or not with marked and characteristic cytotoxic effects of 7KC, 24S-OHC and C24:0. Notably, on 158N cells, there was a marked correlation between Kv3.1b and the mitochondrial depolarization, $O_2^{\bullet-}$ overproduction and plasma membrane damages under treatment with 7KC and 24S-OHC; with C24:0, in the absence of modulation of Kv3.1, no significant correlations have been shown. In BV-2 cells after 24 h, whatever the compound considered no significant modulation of Kv3.1b level was detected. However, with 24S-OHC, a significant positive correlation was observed between Kv3.1b level and the different parameters analyzed (percentage of $DiOC_6(3)$ negative cells, DHE positive cells, and PI positive cells); with 7KC and C24:0 a positive correlation was only found between Kv3.1b leveland the percentage of $DiOC_6$ (3) negative cells. On BV-2 cells, after 48 h, mitochondrial depolarization, $O_2^{\bullet-}$ overproduction and cell death are strongly correlated with Kv3.1b level in presence of 7KC and 24S-OHC. Altogether, these findings may provide evidence for a mechanistic link between Kv3.1b level was detected. However, with 24S-OHC, a significant positive correlation was observed between Kv3.1b level and the different parameters analyzed (percentage of $DiOC_6(3)$ negative cells, DHE positive cells, and PI positive cells); with 7KC and C24:0 a positive correlation was only found between Kv3.1b level and the percentage of $DiOC_6$ (3) negative cells. On BV-2 cells, after 48 h, mitochondrial depolarization, $O_2^{\bullet-}$ overproduction and cell death are strongly correlated with Kv3.1b level in presence of 7KC and 24S-OHC. Altogether, these findings may provide evidence for a mechanistic link between Kv3.1blevel, mitochondrial depolarization and oxidative stress in 158N oligodendrocyte in the presence of 7KC and 24S-OHC, and in BV-2 microglial cells in presence of oxysterols (7KC and 24S-OHC) and C24:0.

The idea that K^+ channels play an important role in the ionic regulation of cell death has already been reported [**99, 100**]. It has been described that modulation of K^+ channel activities by

84]. It has also been reported that $O_2^{\bullet-}$ overproduction can reduce Kv channel activity [**86, 87, 101**]. In addition, it was documented that oxysterols, depending on the nature and location of the oxygen substitution, have distinct impacts on the biophysical properties of membranes, including the formation of liquid ordered domains [**102**]. This supports the notion that the effects of oxysterols on the biophysical properties of the plasma membrane could explain, at least in part, some of their biological activities on Kv3.1b. It was reported that at least 14 species of K^+ channels are involved in apoptosis of various cells [**99**]. An increase in the integral permeability of K^+ channels is conventionally associated with the opening of channels leading to hyperpolarization of apoptotic cells, whereas depolarization was mostly observed [**100**, **103**, **104**]. Perturbation of cellular K^+ homeostasis could be a common motif in apoptosis; increase of intracellular K^+ level, induced by valinomycin, have also been associated with autophagy in BV-2 cells [**105**]. Studies, which describe the mode of valinomycin-induced cell death, report cell shrinkage [**106, 107**], chromatin condensation [**107**], fragmentation of the nucleus [**108**], pyknotic nuclei [**106**], internucleosomal DNA fragmentation in several nerve cell lines (BV-2, C6 rat glioma cells) and in primary mouse astrocytes and microglia cells. Currently, the cytotoxic effects of 7KC and 24S-OHC are associated with oxiapoptophagy (OXIdation, APOPTOsis, and autoPHAGY) in 158N and BV-2 cells [**66, 109**]. Depending on the cell line, oxiapoptophagy is associated or not with modulation of Ca^{2+} homeostasis [**41, 110**]. However, the impact of 7KC, 24S-OHC and C24:0 on the intracellular K^+ homeostasis is unknown. Our data establish that these compounds increased $[K^+]i$ in a dose-dependent manner in 158N and BV-2 cells. The highest intracellular K^+ levels were detected on 158N cells in presence of 7KC, 24S-OHC and C24:0 cells and is positively correlated with mitochondrial depolarization, excessive production of $O_2^{\bullet-}$ and increased plasma membrane permeability which are associated with lipotoxicity. This

cytotoxic effects. Noteworthy, significant positive correlation between $[K^+]i$ and Kv3.1b level have been also observed suggesting that regulation of K^+ homeostasis in oligodendrocytes and microglial cells could involve Kv3.1b.

These findings provide compelling evidences that modulation of Kv3.1b, and intracellular K^+ level are critically linked to various cytotoxic effects triggered by oxysterols (7KC, 24S-OHC) and C24:0 including oxidative stress, mitochondrial dysfunctions and plasma membrane damages on 158N oligodendrocytes and BV-2 microglial cells (**Fig. 6**). This may provide a mechanistic link to better understand the relationships between K^+ homeostasis, Kv3.1b level, oxidative stress, mitochondrial activity, and plasma membrane damages in oligodendrocyte and microglial cells which are affected in numerous neurodegenerative diseases. These data also support the notion that the lipid environment could affect K^+ channel functionality, and they suggest that increased levels of 7KC, 24S-OHC, and C24:0, which are often found in the body fluids and brain of patients with neurodegenerative disease, could impact nerve impulses and nerve cell functions. Therefore, it can be supposed that the regulation of K^+ homeostasis, could constitute a new pharmacological target to prevent neurodegeneration.

CONFLICT OF INTEREST

The authors have no conflicts of interest to declare.

ACKNOWLEDGEMENTS

This work was presented as a poster at the 7th ENOR Symposium 'Oxysterols and Sterol Derivatives in Health and Disease', September 21-22, 2017, Université catholique de Louvain, Brussels, Belgium. This work was supported by grants from: Univ. Bourgogne (Dijon, France),

and the Departments of Neurology (Prof. Thibault Moreau, University Hospital, Dijon, France; Prof. Jérôme de Sèze, University Hospital, Strasbourg, France). We wish to thank Dr. Afef Bahlous, for his help with flame photometry experimental setting. The technical support of Ms. Nejla Labben is gratefully acknowledged. We also thank Mr Philip Bastable for English corrections.

REFERENCES

[1] W.G. Wood, L. Li, W.E. Müller, G.P. Eckert, Cholesterol as a causative factor in Alzheimer's disease: a debatable hypothesis, J. Neurochem. 129 (2014) 559–572. doi:10.1111/jnc.12637

[2] R.S. Yadav, N.K. Tiwari, Lipid integration in neurodegeneration: an overview of Alzheimer's disease, Mol. Neurobiol. 50 (2014) 168–176. doi:10.1007/s12035-014-8661-5

[3] I. Björkhem, S. Meaney, Brain cholesterol: long secret life behind a barrier, Arterioscler. Thromb. Vasc. Biol. 24 (2004) 806–815. doi:10.1161/01.ATV.0000120374.59826.1b

[4] F.R. Maxfield, I. Tabas, Role of cholesterol and lipid organization in disease, Nature. 438 (2005) 612–621. doi:10.1038/nature04399

[5] F. Panza, A. D'Introno, A.M. Colacicco, C. Capurso, G. Pichichero, S.A. Capurso, A. Capurso, V. Solfrizzi, Lipid metabolism in cognitive decline and dementia, Brain Res Rev. 51 (2006) 275–292. doi:10.1016/j.brainresrev.2005.11.007

[6] E.H. Corder, A.M. Saunders, W.J. Strittmatter, D.E. Schmechel, P.C. Gaskell, G.W. Small, A.D. Roses, J.L. Haines, M.A. Pericak-Vance, Gene dose of apolipoprotein E type 4 allele and the risk of Alzheimer's disease in late onset families, Science. 261 (1993) 921–923. doi:10.1016/j.biochi.2012.09.025

[7] V. Mutemberezi, O. Guillemot-Legris, G.G. Muccioli, Oxysterols: From cholesterol metabolites to key mediators, Prog. Lipid Res. 64 (2016) 152–169. doi:10.1016/j.plipres.2016.09.002

[8] J. Vaya, H.M. Schipper, Oxysterols, cholesterol homeostasis, and Alzheimer disease, J. Neurochem. 102 (2007) 1727–1737. doi:10.1111/j.1471-4159.2007.04689.x

[9] P. Gamba, G. Testa, S. Gargiulo, E. Staurenghi, G. Poli, G. Leonarduzzi, Oxidized cholesterol as the driving force behind the development of Alzheimer's disease, Front

[10] T.M. Jeitner, I. Voloshyna, A.B. Reiss, Oxysterol derivatives of cholesterol in neurodegenerative disorders, Curr. Med. Chem. 18 (2011) 1515–1525.

[11] E.G. Lund, J.M. Guileyardo, D.W. Russell, cDNA cloning of cholesterol 24-hydroxylase, a mediator of cholesterol homeostasis in the brain, Proc. Natl. Acad. Sci. U.S.A. 96 (1999) 7238–7243.

[12] D.W. Russell, R.W. Halford, D.M.O. Ramirez, R. Shah, T. Kotti, Cholesterol 24-hydroxylase: an enzyme of cholesterol turnover in the brain, Annu. Rev. Biochem. 78 (2009) 1017–1040. doi:10.1146/annurev.biochem.78.072407.103859

[13] A. Solomon, V. Leoni, M. Kivipelto, A. Besga, A.R. Oksengård, P. Julin, L. Svensson, L.-O. Wahlund, N. Andreasen, B. Winblad, H. Soininen, I. Björkhem, Plasma levels of 24S-hydroxycholesterol reflect brain volumes in patients without objective cognitive impairment but not in those with Alzheimer's disease, Neurosci. Lett. 462 (2009) 89–93. doi:10.1016/j.neulet.2009.06.073

[14] M. Shafaati, A. Solomon, M. Kivipelto, I. Björkhem, V. Leoni, Levels of ApoE in cerebrospinal fluid are correlated with Tau and 24S-hydroxycholesterol in patients with cognitive disorders, Neurosci. Lett. 425 (2007) 78–82. doi:10.1016/j.neulet.2007.08.014.

[15] J. Popp, S. Meichsner, H. Kölsch, P. Lewczuk, W. Maier, J. Kornhuber, F. Jessen, D. Lütjohann, Cerebral and extracerebral cholesterol metabolism and CSF markers of Alzheimer's disease, Biochem. Pharmacol. 86 (2013) 37–42. doi:10.1016/j.bcp.2012.12.007

[16] D. Lütjohann, A. Papassotiropoulos, I. Björkhem, S. Locatelli, M. Bagli, R.D. Oehring, U. Schlegel, F. Jessen, M.L. Rao, K. von Bergmann, R. Heun, Plasma 24S-hydroxycholesterol (cerebrosterol) is increased in Alzheimer and vascular demented patients, J. Lipid Res. 41 (2000) 195–198.

[17] V. Leoni, T. Masterman, U. Diczfalusy, G. De Luca, J. Hillert, I. Björkhem, Changes in human plasma levels of the brain specific oxysterol 24S-hydroxycholesterol during progression of multiple sclerosis, Neurosci. Lett. 331 (2002) 163–166.

[18] N. Noguchi, Y. Urano, W. Takabe, Y. Saito, New aspects of 24(S)-hydroxycholesterol in modulating neuronal cell death, Free Radic. Biol. Med. 87 (2015) 366–372. doi:10.1016/j.freeradbiomed.2015.06.036

[19] A. Zarrouk, M. Hammami, T. Moreau, G. Lizard, Accumulation of 24S-hydroxycholesterol in neuronal SK-N-BE cells treated with hexacosanoic acid (C26:0): argument in favor of 24S-hydroxycholesterol as a potential biomarker of neurolipotoxicity, Rev. Neurol. (Paris). 171 (2015) 125–129. doi:10.1016/j.neurol.2014.10.016

[20] G. Testa, E. Staurenghi, C. Zerbinati, S. Gargiulo, L. Iuliano, G. Giaccone, F. Fantò, G.

33. doi:10.1016/j.redox.2016.09.001

[21] V. Leoni, D. Lütjohann, T. Masterman, Levels of 7-oxocholesterol in cerebrospinal fluid are more than one thousand times lower than reported in multiple sclerosis, J. Lipid Res. 46 (2005) 191–195. doi:10.1194/jlr.C400005-JLR200

[22] S. Mukhopadhyay, K. Fellows, R.W. Browne, P. Khare, S. Krishnan Radhakrishnan, J. Hagemeier, B. Weinstock-Guttman, R. Zivadinov, M. Ramanathan, Interdependence of oxysterols with cholesterol profiles in multiple sclerosis, Mult. Scler. 23 (2017) 792–801. doi:10.1177/1352458516666187.

[23] T. Nury, A. Zarrouk, K. Ragot, M. Debbabi, J.M. Riedinger, A. Vejux, P. Aubourg, G. Lizard, 7-Ketocholesterol is increased in the plasma of X-ALD patients and induces peroxisomal modifications in microglial cells: Potential roles of 7-ketocholesterol in the pathophysiology of X-ALD, J Steroid Biochem Mol Biol. 169 (2016) 123-136. doi: 10.1016/j.jsbmb.2016.03.037

[24] S. Boenzi, F. Deodato, R. Taurisano, B.M. Goffredo, C. Rizzo, C. Dionisi-Vici, Evaluation of plasma cholestane-3β,5α,6β-triol and 7-ketocholesterol in inherited disorders related to cholesterol metabolism, J. Lipid Res. 57 (2016) 361–367. doi:10.1194/jlr.M061978

[25] M. Romanello, S. Zampieri, N. Bortolotti, L. Deroma, A. Sechi, A. Fiumara, R. Parini, B. Borroni, F. Brancati, A. Bruni, C.V. Russo, A. Bordugo, B. Bembi, A. Dardis, Comprehensive Evaluation of Plasma 7-Ketocholesterol and Cholestan-3β,5α,6β-Triol in an Italian Cohort of Patients Affected by Niemann-Pick Disease due to NPC1 and SMPD1 Mutations, Clin. Chim. Acta. 455 (2016) 39–45. doi:10.1016/j.cca.2016.01.003

[26] A. Zarrouk, A. Vejux, J. Mackrill, Y. O'Callaghan, M. Hammami, N. O'Brien, G. Lizard, Involvement of oxysterols in age-related diseases and ageing processes, Ageing Res. Rev. 18 (2014) 148–162. doi:10.1016/j.arr.2014.09.006

[27] D. Trompier, A. Vejux, A. Zarrouk, C. Gondcaille, F. Geillon, T. Nury, S. Savary, G. Lizard, Brain peroxisomes, Biochimie. 98 (2014) 102–110. doi:10.1016/j.biochi.2013.09.009

[28] Y. Takemoto, Y. Suzuki, R. Horibe, N. Shimozawa, R.J.A. Wanders, N. Kondo, Gas chromatography/mass spectrometry analysis of very long chain fatty acids, docosahexaenoic acid, phytanic acid and plasmalogen for the screening of peroxisomal disorders, Brain Dev. 25 (2003) 481–487.

[29] R.J.A. Wanders, S. Ferdinandusse, P. Brites, S. Kemp, Peroxisomes, lipid metabolism and lipotoxicity, Biochim. Biophys. Acta. 1801 (2010) 272–280. doi:10.1016/j.bbalip.2010.01.001

[30] J. Kou, G.G. Kovacs, R. Höftberger, W. Kulik, A. Brodde, S. Forss-Petter, S.

(2011) 271–283. doi:10.1007/s00401-011-0836-9

[31] P. Brites, H.R. Waterham, R.J.A. Wanders, Functions and biosynthesis of plasmalogens in health and disease, Biochim. Biophys. Acta. 1636 (2004) 219–231. doi:10.1016/j.bbalip.2003.12.010

[32] N.E. Braverman, A.B. Moser, Functions of plasmalogen lipids in health and disease, Biochim. Biophys. Acta. 1822 (2012) 1442–1452. doi:10.1016/j.bbadis.2012.05.008

[33] R.J.A. Wanders, Metabolic functions of peroxisomes in health and disease, Biochimie. 98 (2014) 36–44. doi:10.1016/j.biochi.2013.08.022.

[34] G. Astarita, K.M. Jung, V. Vasilevko, N.V. Dipatrizio, S.K. Martin, D.H. Cribbs, E. Head, C.W. Cotman, D. Piomelli, Elevated stearoyl-CoA desaturase in brains of patients with Alzheimer's disease, PLoS ONE. 6 (2011) e24777. doi:10.1371/journal.pone.0024777

[35] A. Zarrouk, J.M. Riedinger, S.H. Ahmed, S. Hammami, W. Chaabane, M. Debbabi, S. Ben Ammou, O. Rouaud, M. Frih, G. Lizard, M. Hammami, Fatty acid profiles in demented patients: identification of hexacosanoic acid (C26:0) as a blood lipid biomarker of dementia, J. Alzheimers Dis. 44 (2015) 1349–1359. doi:10.3233/JAD-142046

[36] V.K. Senanayake, W. Jin, A. Mochizuki, B. Chitou, D.B. Goodenowe, Metabolic dysfunctions in multiple sclerosis: implications as to causation, early detection, and treatment, a case control study, BMC Neurol. 15 (2015) 154. doi:10.1186/s12883-015-0411-4

[37] P. Schönfeld, G. Reiser, Brain Lipotoxicity of Phytanic Acid and Very Long-chain Fatty Acids. Harmful Cellular/Mitochondrial Activities in Refsum Disease and X-Linked Adrenoleukodystrophy, Aging Dis. 7 (2016) 136–149. doi:10.14336/AD.2015.0823

[38] I. Singh, A. Pujol, Pathomechanisms underlying X-adrenoleukodystrophy: a three-hit hypothesis, Brain Pathol. 20 (2010) 838–844. doi:10.1111/j.1750-3639.2010.00392.x

[39] H. Kölsch, D. Lütjohann, A. Tulke, I. Björkhem, M.L. Rao, The neurotoxic effect of 24-hydroxycholesterol on SH-SY5Y human neuroblastoma cells, Brain Res. 818 (1999) 171–175.

[40] J.J. Mackrill, Oxysterols and calcium signal transduction. Chem. Phys. Lipids 164 (2011) 488–495.

[41] A. Zarrouk, T. Nury, M. Samadi, Y. O'Callaghan, M. Hammami, N.M. O'Brien, G. Lizard, Effects of cholesterol oxides on cell death induction and calcium increase in human neuronal cells (SK-N-BE) and evaluation of the protective effects of docosahexaenoic acid (DHA; C22:6 n-3), Steroids. 99 (2015) 238–247. doi:10.1016/j.steroids.2015.01.018

in age-related macular degeneration?, Biochimie. 127 (2016) 70–78. doi:10.1016/j.biochi.2016.04.014

[43] N. Kruska, P. Schönfeld, A. Pujol, G. Reiser, Astrocytes and mitochondria from adrenoleukodystrophy protein (ABCD1)-deficient mice reveal that the adrenoleukodystrophy-associated very long-chain fatty acids target several cellular energy-dependent functions, Biochim. Biophys. Acta. 1852 (2015) 925–936. doi:10.1016/j.bbadis.2015.01.005

[44] S. Hein, P. Schönfeld, S. Kahlert, G. Reiser, Toxic effects of X-linked adrenoleukodystrophy-associated, very long chain fatty acids on glial cells and neurons from rat hippocampus in culture, Hum. Mol. Genet. 17 (2008) 1750–1761. doi:10.1093/hmg/ddn066

[45] J. Jang, S. Park, H. Jin Hur, H.-J. Cho, I. Hwang, Y. Pyo Kang, I. Im, H. Lee, E. Lee, W. Yang, H.-C. Kang, S. Won Kwon, J.-W. Yu, D.-W. Kim, 25-hydroxycholesterol contributes to cerebral inflammation of X-linked adrenoleukodystrophy through activation of the NLRP3 inflammasome, Nat Commun. 7 (2016) 13129. doi:10.1038/ncomms13129. doi:10.1016/j.bcp.2013.02.028

[46] D. Liu, M. Pitta, J.-H. Lee, B. Ray, D.K. Lahiri, K. Furukawa, M. Mughal, H. Jiang, J. Villarreal, R.G. Cutler, N.H. Greig, M.P. Mattson, The KATP channel activator diazoxide ameliorates amyloid-β and tau pathologies and improves memory in the 3xTgAD mouse model of Alzheimer's disease, J. Alzheimers Dis. 22 (2010) 443–457. doi:10.3233/JAD-2010-101017

[47] S. Hadavi, M.D. Baker, R. Dobson, Sustained-release fampridine in Multiple Sclerosis, Mult Scler Relat Disord. 3 (2014) 17–21. doi:10.1016/j.msard.2013.06.003

[48] L.D. Plant, J.P. Boyle, N.M. Thomas, N.J. Hipkins, E. Benedikz, N.M. Hooper, Z. Henderson, P.F.T. Vaughan, C. Peers, R.F. Cowburn, H.A. Pearson, Presenilin-1 mutations alter K+ currents in the human neuroblastoma cell line, SH-SY5Y, Neuroreport. 13 (2002) 1553–1556.

[49] B. Rudy, C.J. Mc Bain, Kv3 channels: voltage-gated K+ channels designed for high frequency repetitive firing, Trends Neurosci. 24 (2001) 517-526.

[50] R.H. Joho, E.C. Hurlock, The role of Kv3-type potassium channels in cerebellar physiology and behavior, Cerebellum. 8 (2009) 323–333. doi:10.1007/s12311-009-0098-4

[51] Y.-M. Leung, Voltage-gated K+ channel modulators as neuroprotective agents, Life Sci. 86 (2010) 775–780. doi:10.1016/j.lfs.2010.04.004

[52] E. Boda, E. Hoxha, A. Pini, F. Montarolo, F. Tempia, Brain expression of Kv3 subunits during development, adulthood and aging and in a murine model of Alzheimer's disease, J.

[53] S. Franciosi, J.K. Ryu, H.B. Choi, L. Radov, S.U. Kim, J.G. McLarnon, Broad-spectrum effects of 4-aminopyridine to modulate amyloid beta1-42-induced cell signaling and functional responses in human microglia, J. Neurosci. 26 (2006) 11652–11664. doi:10.1523/JNEUROSCI.2490-06.2006

[54] C.J. Luneau, J.B.Williams, J. Marshall, E.S. Levitan, C. Oliva, J.S. Smith, J. Antanavage, K. Folander, R.B. Stein, R. Swanson, Alternative splicing contributes to K+ channel diversity in the mammalian central nervous system, Proc Natl Acad Sci USA. 88 (1991) 3932-3936.

[55] B. Rudy, A. Chow, D. Lau, Y. Amarillo, A. Ozaita, M. Saganich, H. Moreno, M.S. Nadal, R. Hernandez-Pineda, A. Hernandez-Cruz, A. Erisir, C. Leonard, E. Vega-Saenz de Miera, Contributions of Kv3 channels to neuronal excitability, Ann. N. Y. Acad. Sci. 868 (1999) 304–343.

[56] M. Weiser, E. Vega-Saenz de Miera, C. Kentros, H. Moreno, L. Franzen, D. Hillman, H. Baker, B. Rudy, Differential expression of Shaw-related K+ channels in the rat central nervous system, J. Neurosci. 14 (1994) 949–972.

[57] P. Song, L.K. Kaczmarek, Modulation of Kv3.1b potassium channel phosphorylation in auditory neurons by conventional and novel protein kinase C isozymes, J. Biol. Chem. 281 (2006) 15582–15591. doi:10.1074/jbc.M512866200

[58] T. Tanaka, S. Yoshida, Mechanisms of remyelination: recent insight from experimental models, Biomol Concepts. 5 (2014) 289–298. doi:10.1515/bmc-2014-0015

[59] L. Pini, M. Pievani, M. Bocchetta, D. Altomare, P. Bosco, E. Cavedo, S. Galluzzi, M. Marizzoni, G.B. Frisoni, Brain atrophy in Alzheimer's Disease and aging, Ageing Res. Rev. 30 (2016) 25–48. doi:10.1016/j.arr.2016.01.002

[60] N. Baumann, D. Pham-Dinh, Biology of oligodendrocyte and myelin in the mammalian central nervous system, Physiol Rev. 81 (2001) 871-927.

[61] Z. Cai, M. Xiao, Oligodendrocytes and Alzheimer's disease, Int. J. Neurosci. 126 (2016) 97–104. doi:10.3109/00207454.2015.1025778

[62] A.C. Feutz, D. Pham-Dinh, B. Allinquant, M. Miehe, M.S. Ghandour, An immortalized jimpy oligodendrocyte cell line: defects in cell cycle and cAMP pathway, Glia. 34 (2001) 241–252.

[63] M. Baarine, K. Ragot, E.C. Genin, H. El Hajj, D. Trompier, P. Andreoletti, M.S. Ghandour, F. Menetrier, M. Cherkaoui-Malki, S. Savary, G. Lizard, Peroxisomal and mitochondrial status of two murine oligodendrocytic cell lines (158N, 158JP): potential models for the study of peroxisomal disorders associated with dysmyelination processes, J. Neurochem. 111 (2009) 119–131. doi:10.1111/j.1471-4159.2009.06311.x

Barros, A. Vejux, J.-M. Riedinger, D. Delmas, G. Lizard, Absence of correlation between oxysterol accumulation in lipid raft microdomains, calcium increase, and apoptosis induction on 158N murine oligodendrocytes, Biochem. Pharmacol. 86 (2013) 67–79.

[65] M. Baarine, P. Andreoletti, A. Athias, T. Nury, A. Zarrouk, K. Ragot, A. Vejux, J.-M. Riedinger, Z. Kattan, G. Bessede, D. Trompier, S. Savary, M. Cherkaoui-Malki, G. Lizard, Evidence of oxidative stress in very long chain fatty acid--treated oligodendrocytes and potentialization of ROS production using RNA interference-directed knockdown of ABCD1 and ACOX1 peroxisomal proteins, Neuroscience. 213 (2012) 1–18. doi:10.1016/j.neuroscience.2012.03.058

[66] T. Nury, A. Zarrouk, J.J. Mackrill, M. Samadi, P. Durand, J.M.Riedinger, M. Doria, A. Vejux, E. Limagne, D. Delmas, M. Prost, T. Moreau, M. Hammami, R. Delage-Mourroux, N.M.O'Brien, G. Lizard, Induction of oxiapoptophagy on 158N murine oligodendrocytes treated by 7-ketocholesterol-, 7β-hydroxycholesterol-, or 24(S)-hydroxycholesterol: Protective effects of α-tocopherol and docosahexaenoic acid (DHA; C22:6 n-3), Steroids. 99 (2015) 194–203

[67] A. Zarrouk, T. Nury, A. Dauphin, P. Frère, J.-M. Riedinger, C.-M. Bachelet, F. Frouin, T. Moreau, M. Hammami, E. Kahn, G. Lizard, Impact of C24:0 on actin-microtubule interaction in human neuronal SK-N-BE cells: evaluation by FRET confocal spectral imaging microscopy after dual staining with rhodamine-phalloidin and tubulin tracker green, Funct. Neurol. 30 (2015) 33–46

[68] M. Bezine, M. Debbabi, T. Nury, R. Ben-Khalifa, M. Samadi, M. Cherkaoui-Malki, A. Vejux, Q. Raas, J. de Sèze, T. Moreau, M. El-Ayeb, G. Lizard, Evidence of K(+) homeostasis disruption in cellular dysfunction triggered by 7-ketocholesterol, 24S-hydroxycholesterol, and tetracosanoic acid (C24:0) in 158N murine oligodendrocytes, Chem Phys Lipids. 207 (2017) 135-150. doi: 10.1016/j.chemphyslip.2017.03.006

[69] G. Rothe, G. Valet, Flow cytometric analysis of respiratory burst activity in phagocytes with hydroethidine and 2',7'-dichlorofluorescin, J. Leukoc. Biol. 47 (1990) 440–448.

[70] G. Lizard, S. Fournel, L. Genestier, N. Dhedin, C. Chaput, M. Flacher, M. Mutin, G. Panaye, J.P. Revillard, Kinetics of plasma membrane and mitochondrial alterations in cells undergoing apoptosis, Cytometry. 21 (1995) 275–283. doi:10.1002/cyto.990210308

[71] A. Ozaita, M.E. Martone, M.H. Ellisman, B. Rudy, Differential subcellular localization of the two alternatively spliced isoforms of the Kv3.1 potassium channel subunit in brain, J. Neurophysiol. 88 (2002) 394–408

[72] J. Abdel-Khalik, E. Yutuc, P.-J.Crick, J.-Å. Gustafsson, M.Warner, G. Roman, K. Talbot, E. Gray, W.J.Griffiths, M.R.Turner, Wang Y.J, Defective cholesterol metabolism in amyotrophic lateral sclerosis, Lipid Res. 1 (2017) 267-278. doi: 10.1194/jlr.P071639

charge-tags for sterol and oxysterol analysis, Clin Chem. 2 (2015) 400-411. doi: 10.1373/clinchem.2014.231332

[74] I. Björkhem, Crossing the barrier: oxysterols as cholesterol transporters and metabolic modulators in the brain, J. Intern. Med. 260 (2006) 493–508. doi:10.1111/j.1365-2796.2006.01725.x

[75] J.R. Hascalovici, J. Vaya, S. Khatib, C.A. Holcroft, H. Zukor, W. Song, Z. Arvanitakis, D.A. Bennett, H.M. Schipper, Brain sterol dysregulation in sporadic AD and MCI: relationship to heme oxygenase-1, J. Neurochem. 110 (2009) 1241–1253. doi:10.1111/j.1471-4159.2009.06213.x

[76] V. Leoni, C. Caccia, 24S-hydroxycholesterol in plasma: a marker of cholesterol turnover in neurodegenerative diseases, Biochimie. 95 (2013) 595–612

[77] P.J. Crick, W.J. Griffiths, J. Zhang, M. Beibel, J. Abdel-Khalik, J. Kuhle, A.W. Sailer, Y. Wang, Reduced Plasma Levels of 25-Hydroxycholesterol and Increased Cerebrospinal Fluid Levels of Bile Acid Precursors in Multiple Sclerosis Patients, Mol. Neurobiol. (2016). doi:10.1007/s12035-016-0281-9

[78] S. Zhornitsky, K.A. McKay, L.M. Metz, C.E. Teunissen, M. Rangachari, Cholesterol and markers of cholesterol turnover in multiple sclerosis: relationship with disease outcomes, Mult Scler Relat Disord. 5 (2016) 53–65. doi:10.1016/j.msard.2015.10.005

[79] M. Doria, L. Maugest, T. Moreau, G. Lizard, A. Vejux, Contribution of cholesterol and oxysterols to the pathophysiology of Parkinson's disease, Free Radic. Biol. Med. 101 (2016) 393–400. doi:10.1016/j.freeradbiomed.2016.10.008

[80] F. Kreilaus, A.S. Spiro, C.A. McLean, B. Garner, A.M. Jenner, Evidence for altered cholesterol metabolism in Huntington's disease post mortem brain tissue, Neuropathol. Appl. Neurobiol. 42 (2016) 535–546. doi:10.1111/nan.12286

[81] A.M. Petrov, M.R. Kasimov, A.L. Zefirov, Brain Cholesterol Metabolism and Its Defects: Linkage to Neurodegenerative Diseases and Synaptic Dysfunction, Acta Naturae. 8 (2016) 58–73.

[82] F.D. Porter, D.E. Scherrer, M.H. Lanier, S.J. Langmade, V. Molugu, S.E. Gale, D. Olzeski, R. Sidhu, D.J. Dietzen, R. Fu, C.A. Wassif, N.M. Yanjanin, S.P. Marso, J. House, C. Vite, J.E. Schaffer, D.S. Ory, Cholesterol oxidation products are sensitive and specific blood-based biomarkers for Niemann-Pick C1 disease, Sci Transl Med. 2 (2010) 56ra81. doi:10.1126/scitranslmed.3001417

[83] T. Wei, M. Yi, W. Gu, L. Hou, Q. Lu, Z. Yu, H. Chen, The potassium channel KCa3.1 represents a valid pharmacological target for astrogliosis-induced neuronal impairment in a mouse model of Alzheimer's disease, Front Pharmacol. 7 (2016) 528.

[84] F. Sesti, Oxidation of K(+) channels in aging and neurodegeneration, Aging Dis. 7 (2016) 130–135. doi:10.14336/AD.2015.0901

[85] S.-Q. Cai, F. Sesti, Oxidation of a potassium channel causes progressive sensory function loss during aging, Nat. Neurosci. 12 (2009) 611–617. doi:10.1038/nn.2291

[86] D. Cotella, B. Hernandez-Enriquez, X. Wu, R. Li, Z. Pan, J. Leveille, C.D. Link, S. Oddo, F. Sesti, Toxic role of K+ channel oxidation in mammalian brain, J. Neurosci. 32 (2012) 4133–4144. doi:10.1523/JNEUROSCI.6153-11.2012

[87] Y.-H. Wu, D. Arnaud-Cormos, M. Casciola, J.M. Sanders, P. Leveque, P.T. Vernier, Moveable wire electrode microchamber for nanosecond pulsed electric-field delivery, IEEE Trans Biomed Eng. 60 (2013) 489–496. doi:10.1109/TBME.2012.2228650

[88] J.R. Yaron, S. Gangaraju, M.Y. Rao, X. Kong, L. Zhang, F. Su, Y. Tian, H.L. Glenn, D.R. Meldrum, K(+) regulates Ca(2+) to drive inflammasome signaling: dynamic visualization of ion flux in live cells, Cell Death Dis. 6 (2015) e1954. doi:10.1038/cddis.2015.277.

[89] K. Kunzelmann, Ion channels in regulated cell death, Cell. Mol. Life Sci. 73 (2016) 2387–2403. doi:10.1007/s00018-016-2208-z

[90] U.B. Evo, M.E. Dailey. Microglia: key elements in neural development, plasticity, and pathology. J Neuroimmune Pharmacol. 8 (2013) 494–509.

[91] B. Ettle, J.C.M. Schlachetzki, J. Winkler. Oligodendroglia and myelin in neurodegenerative diseases: more than just bystanders? Mol. Neurobiol. 53 (2016) 3046–3062. doi:10.1007/s12035-015-9205-3.

[92] T.M. Perney, J. Marshall, K.A. Martin, S. Hockfield, L.K. Kaczmarek, Expression of the mRNAs for the Kv3.1 potassium channel gene in the adult and developing rat brain, J. Neurophysiol. 68 (1992) 756–766.

[93] S. Tiwari-Woodruff, L. Beltran-Parrazal, A. Charles, T. Keck, T. Vu, J. Bronstein, K+ channel KV3.1 associates with OSP/claudin-11 and regulates oligodendrocyte development. Am. J. Physiol. Cell Physiol. 291 (2006) C687-698. doi:10.1152/ajpcell.00510.2005

[94] C.-Y. Wu, C. Kaur, V. Sivakumar, J. Lu, E.-A. Ling, Kv1.1 expression in microglia regulates production and release of proinflammatory cytokines, endothelins and nitric oxide. Neuroscience. 158 (2009) 1500–1508. doi:10.1016/j.neuroscience.2008.11.043

[95] A. Vejux, S. Guyot, T. Montange, J.-M.Riedinger, E. Kahn, G. Lizard, Phospholipidosis and down-regulation of the PI3-K/PDK-1/Akt signalling pathway are vitamin E inhibitable

[96] M. Debbabi, A. Zarrouk, M. Bezine, W. Meddeb, T. Nury, A. Badreddine, E.-M. Karym, R. Sghaier, L. Bretillon, S. Guyot, M. Samadi, M. Cherkaoui-Malki, B. Nasser, M. Mejri, S. Ben-Hammou, M. Hammami, G. Lizard, Comparison of the effects of major fatty acids present in the Mediterranean diet (oleic acid, docosahexaenoic acid) and in hydrogenated oils (elaidic acid) on 7-ketocholesterol-induced oxiapoptophagy in microglial BV-2 cells, Chem Phys Lipids. 207 (2017) 151-170. doi: 10.1016/j.chemphyslip.2017.04.002

[97] V.M. Olkkonen, R. Hynynen, Interactions of oxysterols with membranes and proteins, Mol Aspects Med. 3 (2009) 123-33. doi: 10.1016/j.mam.2009.02.004

[98] C.D. Stubbs, A.-D. Smith, Essential fatty acids in membrane: physical properties and function, Biochem Soc Trans. 5 (1990) 779-81. doi: 10.1042/bst0180779

[99] S.P. Yu, Regulation and critical role of potassium homeostasis in apoptosis, Prog Neurobiol. 70 (2003) 363-386.

[100] C.D. Bortner, M. Gomez-Angelats, J.A. Cidlowski, Plasma membrane depolarization without repolarization is an early molecular event in anti-Fas-induced apoptosis, J. Biol. Chem. 276 (2001) 4304–4314. doi:10.1074/jbc.M005171200

[101] S.Q. Cai, F. Sesti, Oxidation of a potassium channel causes progressive sensory function loss during aging, Nat. Neurosci. 12 (2009) 611–617. doi:10.1038/nn.2291

[102] V.M. Olkkonen, R. Hynynen, Interactions of oxysterols with membranes and proteins, Mol. Aspects Med. 30 (2009) 123–133. doi:10.1016/j.mam.2009.02.004

[103] R. Franco, C.D. Bortner, J.A. Cidlowski, Potential roles of electrogenic ion transport and plasma membrane depolarization in apoptosis, J. Membr. Biol. 209 (2006) 43–58. doi:10.1007/s00232-005-0837-5

[104] C.D. Bortner, J.A. Cidlowski, Cell shrinkage and monovalent cation fluxes: role in apoptosis, Arch. Biochem. Biophys. 462 (2007) 176–188. doi:10.1016/j.abb.2007.01.020

[105] B. Klein, K. Wörndl, U. Lütz-Meindl, H.H. Kerschbaum, Perturbation of intracellular K(+) homeostasis with valinomycin promotes cell death by mitochondrial swelling and autophagic processes, Apoptosis. 16 (2011) 1101–1117. doi:10.1007/s10495-011-0642-9

[106] Y. Inai, M. Yabuki, T. Kanno, J. Akiyama, T. Yasuda, K. Utsumi, Valinomycin induces apoptosis of ascites hepatoma cells (AH-130) in relation to mitochondrial membrane potential, Cell Struct. Funct. 22 (1997) 555–563.

[107] S.P. Yu, C.H. Yeh, S.L. Sensi, B.J. Gwag, L.M. Canzoniero, Z.S. Farhangrazi, H.S. Ying, M. Tian, L.L. Dugan, D.W. Choi, Mediation of neuronal apoptosis by enhancement of outward potassium current, Science. 278 (1997) 114–117.

apoptosis induced by methylprednisolone and valinomycin analyzed by flow cytometry, Exp. Cell Res. 208 (1993) 362–370. doi:10.1006/excr.1993.1257

[109] T. Nury, A. Zarrouk, A. Vejux, M. Doria, J.M. Riedinger, R. Delage-Mourroux, G. Lizard, Induction of oxiapoptophagy, a mixed mode of cell death associated with oxidative stress, apoptosis and autophagy, on 7-ketocholesterol-treated 158N murine oligodendrocytes: impairment by α-tocopherol, Biochem. Biophys. Res. Commun. 446 (2014) 714–719. doi:10.1016/j.bbrc.2013.11.081

[110] A. Vejux, G. Lizard, Cytotoxic effects of oxysterols associated with human diseases: Induction of cell death (apoptosis and/or oncosis), oxidative and inflammatory activities, and phospholipidosis, Mol. Aspects Med. 30 (2009) 153–170. doi:10.1016/j.mam.2009.02.006

FIGURE LEGENDS

Fig. 1. Analysis of the expression of the Kv3.1 voltage-gated potassium channel in 158N murine oligodendrocytes and BV-2 murine microglial cells. A: Flow cytometric analysis of the expression of Kv3.1 on 158N and BV-2 cells; **B**: immunofluorescence microscopy; Kv3.1 expression (green); the nuclei were counterstained with Hoechst 33342 (blue); **C**: analysis of Kv3.1b protein expression by Western blot in 158N and BV-2 cells; a single band at around 66 kDa corresponding to the core Kv3.1b was detected.

Fig. 2. Analysis of Kv3.1b level in 158N murine oligodendrocytes treated with 7KC, 24S-OHC and C24:0. Subconfluent 158N cells (previously cultured for 24 h) were further incubated for 24 h without or with 7KC (2.5 to 25 µM), 24S-OHC (2.5 to 25 µM), and C24:0 (1 to 20 µM) as well as with EtOH (0.005 to 0.05%; used as vehicle for 7KC and 24S-OHC) and with α-cyclodextrin (0.05 to 1 mM; used as vehicle for C24:0). Kv3.1b level was evaluated by flow cytometry (data were expressed as % of control (untreated cells)) (**A**) and western blotting (data were normalized to β-actin used as reference protein and expressed as % control) (**B**). Data shown are mean ± SD from three independent experiments. Statistical analyses were realized

oxysterols or tetracosanoic acid / vehicle.

Fig. 3. Analysis of Kv3.1b level in BV-2 murine microglial cells treated with 7KC, 24S-OHC and C24:0. BV-2 cells previously cultured for 24 h were further incubated for 24 and 48 h without or with 7KC (2.5 to 25 µM), 24S-OHC (2.5 to 25 µM) and C24:0 (1 to 20 µM) as well as with EtOH (0.005 to 0.05%; used as vehicle for 7KC and 24S-OHC) and with α-cyclodextrin (0.05 to 1 mM; used as vehicle for C24:0). Kv3.1b level (MFI) was evaluated by flow cytometry after 24 h (**A**) and 48 h (**B**). Data are expressed as % of control (untreated cells). Data shown are mean ± SD from three independent experiments. Statistical analyses were realized with ANOVA (Tukey's multiple comparisons test): # $P < 0.05$ vehicle / control; * $P < 0.05$ oxysterols or tetracosanoic acid / vehicle.

Fig. 4. Effects of 7KC, 24S-OHC and C24:0 on intracellular K^+ concentration ($[K^+]i$) evaluated with flame photometry. 158N and BV-2 cells previously cultured for 24 h were further cultured without or with 7KC (2.5 to 25 µM), 24S-OHC (2.5 to 25 µM), and C24:0 (1 to 20 µM) as well as with EtOH (0.005 to 0.05%; used as vehicle for 7KC and 24S-OHC) and with α-cyclodextrin (0.05 to 1 mM; used as vehicle for C24:0). 4-AP was used as positive control to induce intracellular K+ accumulation. $[K^+]i$ was measured by flame photometry after 24 h of treatment in 158N cells (**A**), or after 24 h (**B**) and 48 h of treatment (**C**) in BV-2 cells. Data are expressed as % of control (untreated cells). Values are mean ± SD of three independent experiments. Statistical analyses were realized with ANOVA (Tukey's multiple comparisons test). Significant differences are indicated as: # $P < 0.05$ vehicle (or 4-AP) / control; * $P < 0.05$, vehicle / 7KC, 24S-OHC or C24:0.

([K^+]i) evaluated in 158 N murine oligodendrocytes and BV-2 murine microglial cells treated with 7KC, 24S-OHC or C24:0. 158N (**a-c**) and BV-2 (**d-i**) cells previously cultured for 24 h were further cultured (for 24 h (158N) or 24-48 h (BV-2)) without or with 7KC (2.5 to 25 µM), 24S-OHC (2.5 to 25 µM), and C24:0 (1 to 20 µM)as well as with EtOH (0.005 to 0.05 %; used as vehicle for 7KC and 24S-OHC) and with α-cyclodextrin (0.05 to 1 mM; used as vehicle for C24:0). Kv3.1b levellevel was evaluated by flow cytometry (MFI) and [K^+]i was determined by flame photometry. Data are expressed as % of control (untreated cells). The correlations were calculated with the Pearson's correlation test.

Fig. 6. Shematic representation of the contribution of Kv3.1 in 7KC -, 24S-OHC - and C24:0 - induced cell death. Under treatment with 7KC, 24S-OHC and C24:0, an increased of the intracellular K^+ concentration [K^+]i is observed associated with plasma membrane changes, ROS overproduction and loss of transmembrane mitochondrial potential (ΔΨm). Under treatment with 7KC and 24S-OHC, an overpression of Kv3.1, that could set up to prevent the increase of [K+]i, is observed. However, in the presence of C24:0, no increase of Kv3.1 level occurs. This finding provides evidence for a potential link between Kv3.1 level (mainly Kv3.1b), intracellular K^+ accumulation and cell death induction in the presence of 7KC, 24S-OHC and C24:0. However, our data also show that 7KC, 24S-OHC and C24:0 simultaneously activate P2X7 receptor which leads to Na^+ and Ca^{2+} influx, and K^+ efflux. It is therefore questionable whether the increased [K^+]i under the action of 7KC, 24S-OHC and C24:0 could be the resultant of several concomitant activities of these molecules on different targets involved in the control of K^+ homeostasis.

Prof. William J. Griffiths and Dr Yuqin Wang, Univ. Swansea, UK)

Supplementary Figure 2: Pearson's correlation between Kv3.1b level, the percentage of $DiOC_6(3)$-negative cells, and DHE- and PI-positive cells in 158N murine oligodendrocytes treated for 24 h with 7-ketocholesterol, 24S-hydroxycholesterol or C24:0. Sub-confluent 158N cells (previously cultured for 24 h) were further incubated for 24 h without or with 7KC (2.5 to 25 µM), 24S-OHC (2.5 to 25 µM), and C24:0 (1 to 20 µM) as well as with EtOH (0.005 to 0.05%; used as vehicle for 7KC and 24S-OHC) and with α-cyclodextrin (0.05 to 1 mM; used as vehicle for C24:0). Kv3.1b level (MFI) as well as the percentage $DiOC_6(3)$-negative cells, and DHE- and PI-positive cells were evaluated by flow cytometry. The correlations were calculated with the Pearson's correlation test.

Supplementary Figure 3: Pearson's correlation between Kv3.1b level, the percentage of $DiOC_6(3)$-negative cells, and DHE- and PI-positive cells in BV-2 murine microglial cells treated for 24 h with 7-ketocholesterol, 24S-hydroxycholesterol or C24:0. BV-2 cells (previously cultured for 24 h) were further incubated for 24 h without or with 7KC (2.5 to 25 µM), 24S-OHC (2.5 to 25 µM), and C24:0 (1 to 20 µM)as well as with EtOH (0.005 to 0.05%; used as vehicle for 7KC and 24S-OHC) and with α-cyclodextrin (0.05 to 1 mM; used as vehicle for C24:0). Kv3.1b level (MFI) as well as the percentage of $DiOC_6(3)$-negative cells, and DHE- and PI-positive cells were evaluated by flow cytometry. The correlations were calculated with the Pearson's correlation test.

$DiOC_6(3)$-negative cells, and DHE- and PI-positive cells in BV-2 murine microglial cells cultured for 48 h with 7-ketocholesterol, 24S-hydroxycholesterol or C24:0. BV-2 cells (previously cultured for 24 h) were further cultured for 48 h without or with 7KC (2.5 to 25 µM), 24S-OHC (2.5 to 25 µM), and C24:0 (1 to 20 µM) as well as with EtOH (0.005 to 0.05%; used as vehicle for 7KC and 24S-OHC) and with α-cyclodextrin (0.05 to 1 mM; used as vehicle for C24:0). Kv3.1b level (MFI) as well as the percentage $DiOC_6(3)$-negative cells, and DHE- and PI-positive cells were evaluated by flow cytometry. The correlations were calculated with Pearson's correlation test.

Supplementary Figure 5: Pearson's correlation between intracellular K^+ concentration ($[K^+]i$), the percentage of $DiOC_6(3)$-negative cells, and DHE- and PI-positive cells in 158 N murine oligodendrocytes cultured for 24 h with 7-ketocholesterol, 24S-hydroxycholesterol or C24:0. Subconfluent 158N cells (previously cultured for 24 h) were further cultured for 24 h without or with 7KC (2.5 to 25 µM), 24S-OHC (2.5 to 25 µM), and C24:0 (1 to 20 µM) as well as with EtOH (0.005 to 0.05%; used as vehicle for 7KC and 24S-OHC) and with α-cyclodextrin (0.05 to 1 mM; used as vehicle for C24:0). $[K^+]i$ was determined by flame photometry; the percentages of $DiOC_6(3)$-negative cells, and DHE- and PI-positive cells were evaluated by flow cytometry. The correlations were calculated with Pearson's correlation test.

Supplementary Figure 6: Pearson's correlation between intracellular K^+ concentration ($[K^+]i$), the percentage of $DiOC_6(3)$-negative cells, and DHE- and PI-positive cells in BV-2 murine microglial cells treated for 24 h with 7-ketocholesterol, 24S-hydroxycholesterol or C24:0. BV-2 cells (previously cultured for 24 h) were further cultured for 24 h without or with

(0.005 to 0.05%; used as vehicle for 7KC and 24S-OHC) and with α-cyclodextrin (0.05 to 1 mM; used as vehicle for C24:0). $[K^+]i$ was determined by flame photometry; the percentages of $DiOC_6(3)$-negative cells, and DHE- and PI-positive cells were evaluated by flow cytometry. The correlations were calculated with Pearson's correlation test.

<u>Supplementary Figure 7:</u> Pearson's correlation between intracellular K^+ concentration ($[K^+]i$), the percentage of $DiOC_6(3)$-negative cells, and DHE- and PI-positive cells in BV-2 murine microglial cells treated for 48 h with 7-ketocholesterol, 24S-hydroxycholesterol or C24:0. BV-2 cells (previously cultured for 24 h) were further cultured for 48 h without or with 7KC (2.5 to 25 µM), 24S-OHC (2.5 to 25 µM), and C24:0 (1 to 20 µM) as well as with EtOH (0.005 to 0.05%; used as vehicle for 7KC and 24S-OHC) and with α-cyclodextrin (0.05 to 1 mM; used as vehicle for C24:0). $[K^+]i$ was determined by flame photometry; the percentages of $DiOC_6(3)$-negative cells, and DHE- and PI-positive cells were evaluated by flow cytometry. The correlations were calculated with Pearson's correlation test.

Graphical abstract

Our data establish that 7KC, 24S-OHC and C24:0 increase intracellular K^+ concentration ($[K^+]i$) in both 158N and BV-2 cells. The highest $[K^+]i$ were detected on 158N cells. Increased level of Kv3.1b was shown on 158N cells under treatment with 7KC and 24S-OHC but not with C24:0. This effect was less important on BV-2 cells. Positive correlations between Kv3.1b level and $[K^+]i$ were observed. In addition, the $[K^+]i$ and the level of Kv3.1b along with increasing percentage cells with depolarized mitochondria, ROS overproducing cells and dead cells.

158N (24 h)	**7KC**	0.8	0.0002	0.91	<0.0001	0.75	0.0007
	24 S-OHC	0.95	<0.0001	0.85	<0.0001	0.9	<0.0001
	C24:0	0.2	NS	-0.05	NS	0.11	NS
BV-2 (24 h)	**7KC**	0.73	0.0013	0.42	NS	0.4	NS
	24 S-OHC	0.55	0.02	0.71	0.0019	0.63	0.0087
	C24:0	0.57	0.007	0.41	NS	0.31	NS
BV-2 (48 h)	**7KC**	0.6	0.01	0.72	0.0015	0.7	0.002
	24 S-OHC	0.79	0.0002	0.79	0.0002	0.7	0.0015
	C24:0	0.2	NS	-0.24	NS	0.032	NS

Table 1: Pearson's correlation between Kv3.1b expression, percentage of $DiOC_6(3)$ negative cells, and percentage of DHE and PI positive cells.

Cells and times of treatment	[K+]i	DiOC6(3) negative cells		DHE positive cells		PI positive cells	
		r	*P*	r	*P*	r	*P*
158N (24 h)	7KC	0.92	<0.0001	0.94	<0.0001	0.81	<0.0001
	24 S-OHC	0.83	<0.0001	0.86	<0.0001	0.86	<0.0001
	C24:0	0.89	<0.0001	0.8	<0.0001	0.8	0.0002
BV-2 (24 h)	7KC	0.73	0.012	0.92	0.0018	0.85	<0.0001
	24 S-OHC	0.86	0.0003	0.71	0.0018	0.89	<0.0001
	C24:0	0.81	0.001	0.64	0.0019	0.84	0.0002
BV-2 (48 h)	7KC	0.49	0.04	0.5	0.03	0.61	0.011
	24 S-OHC	0.06	NS	-0.14	NS	0.03	NS
	C24:0	0.75	<0.0001	0.47	0.033	0.8	<0.0001

Table 2: Pearson's correlation between intracellular potassium concentration [K+]i, percentage of $DiOC_6(3)$ negative cells, and percentage of DHE and PI positive cells.

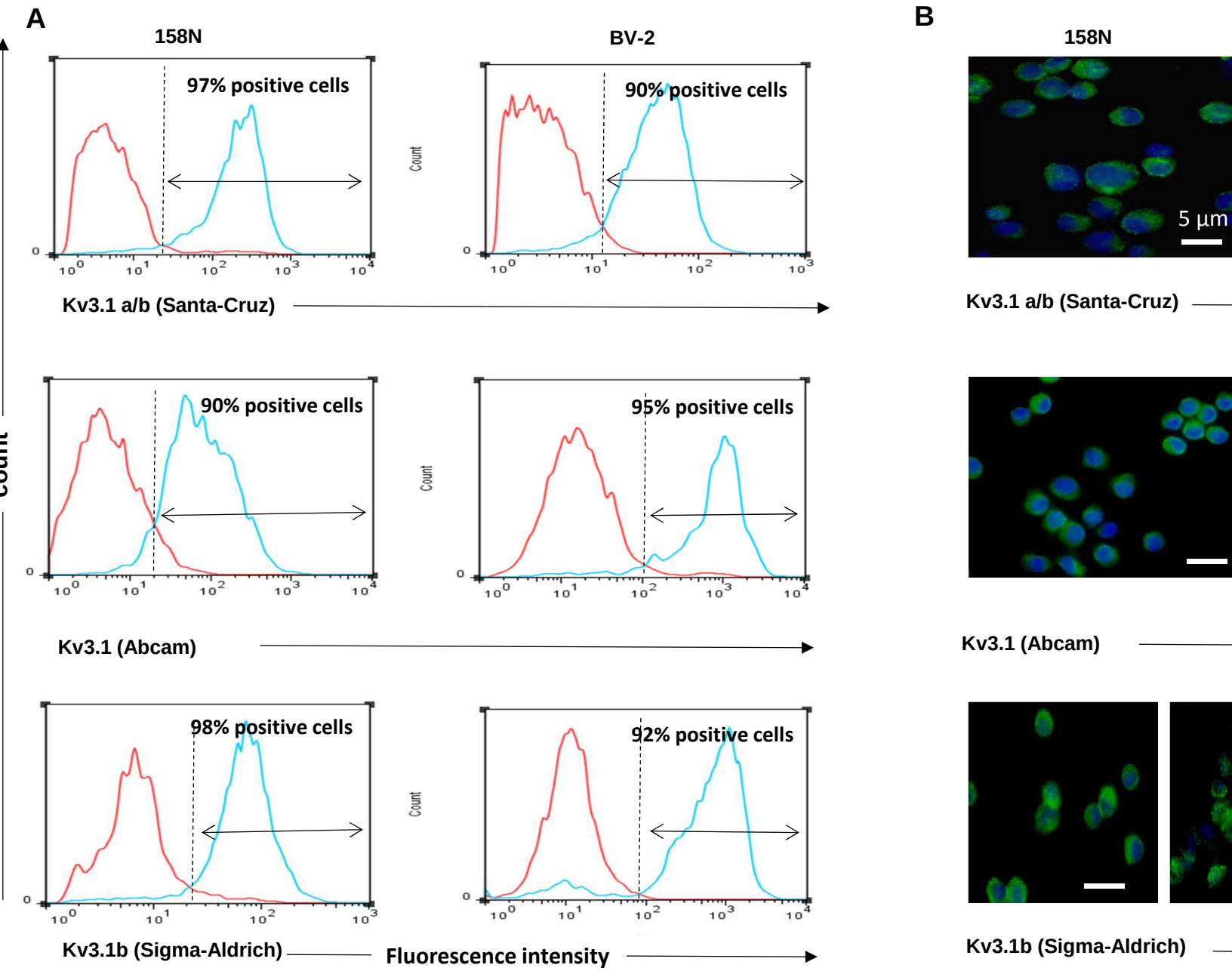

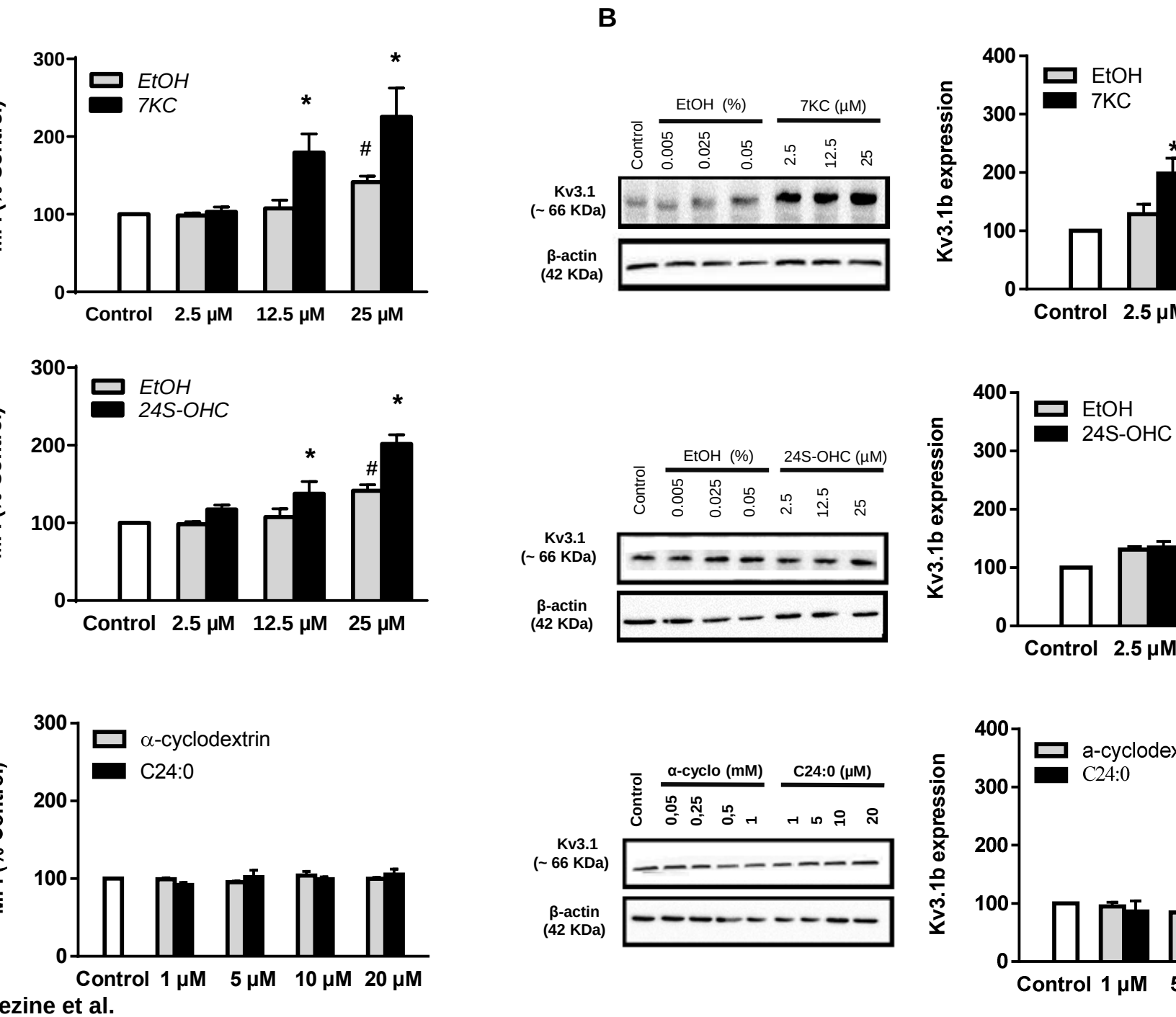
B
EtOH
7KC
Control
2.5 µM
12.5 µM
25 µM
EtOH (%)
7KC (µM)
Control
0.005
0.025
0.05
2.5
12.5
25
Kv3.1
(~ 66 KDa)
β-actin
(42 KDa)
Kv3.1b expression
EtOH
24S-OHC
α-cyclodextrin
C24:0
α-cyclo (mM)
C24:0 (µM)
0,05
0,25
0,5
1
1 µM
5 µM
10 µM
20 µM

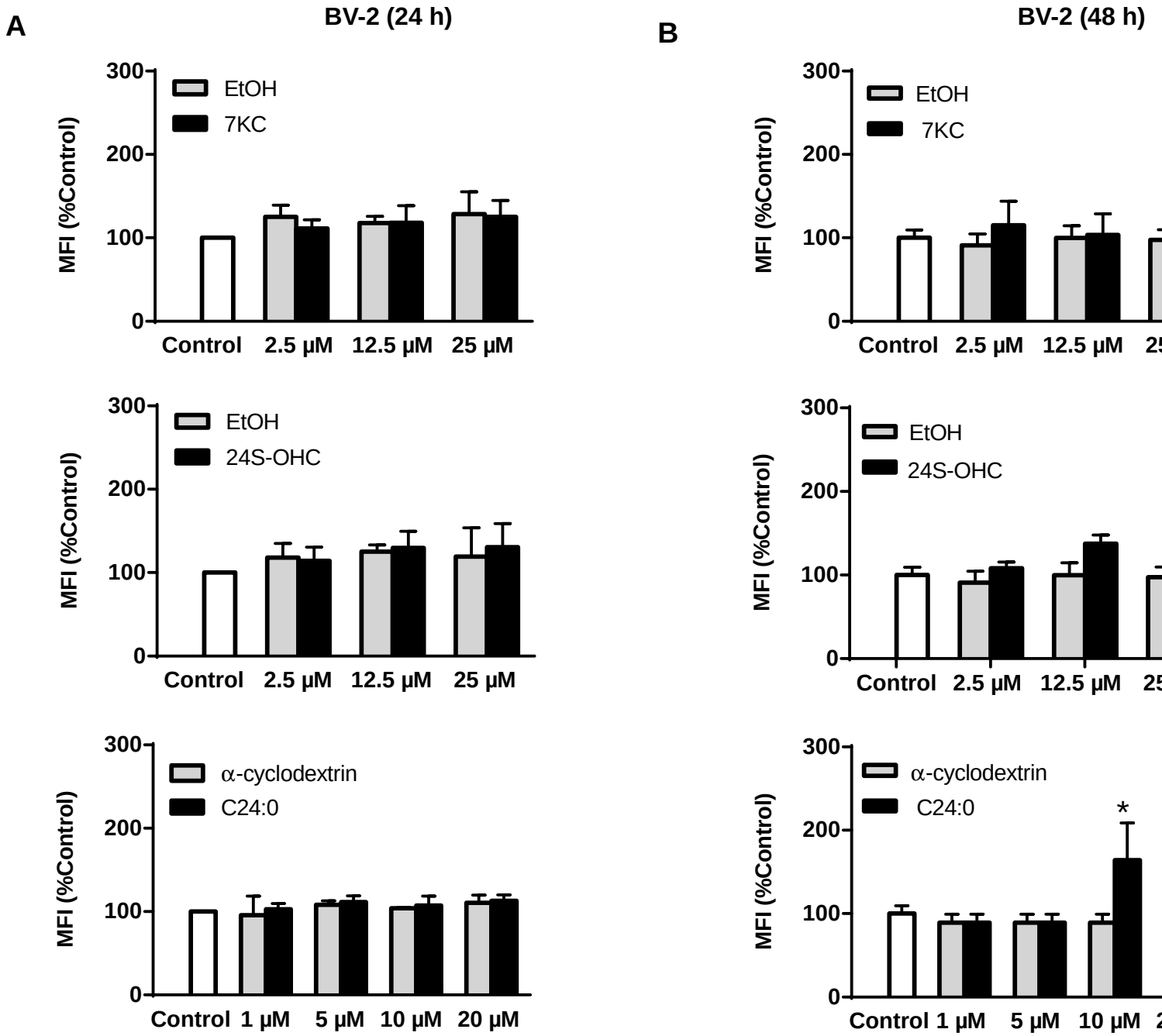
A
BV-2 (24 h)
B
BV-2 (48 h)
MFI (%Control)
EtOH
7KC
24S-OHC
α-cyclodextrin
C24:0
Control
2.5 µM
12.5 µM
25 µM
1 µM
5 µM
10 µM
20 µM
*

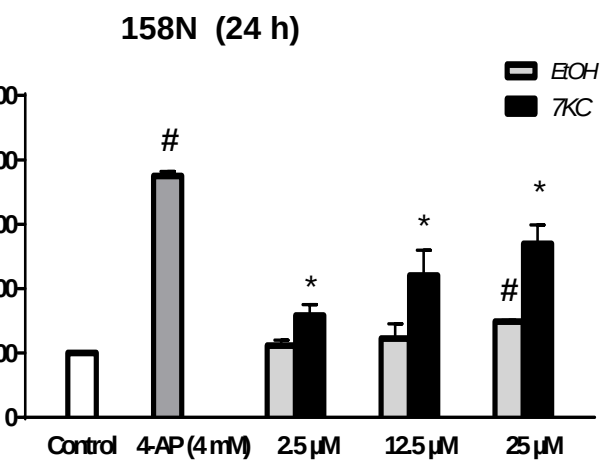

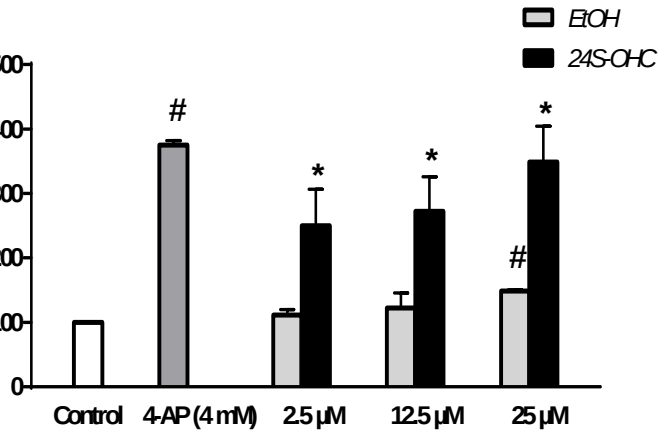

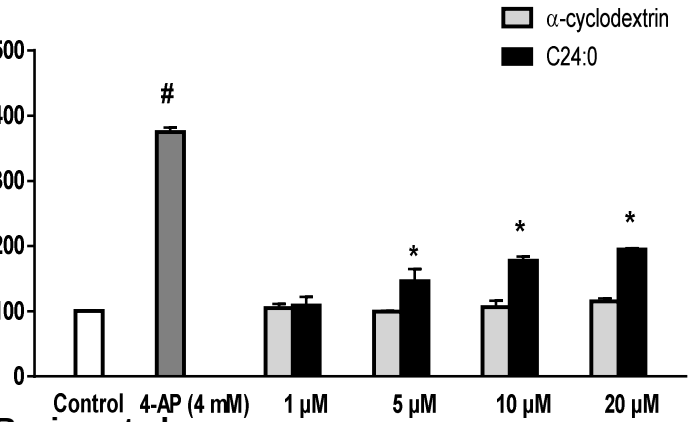

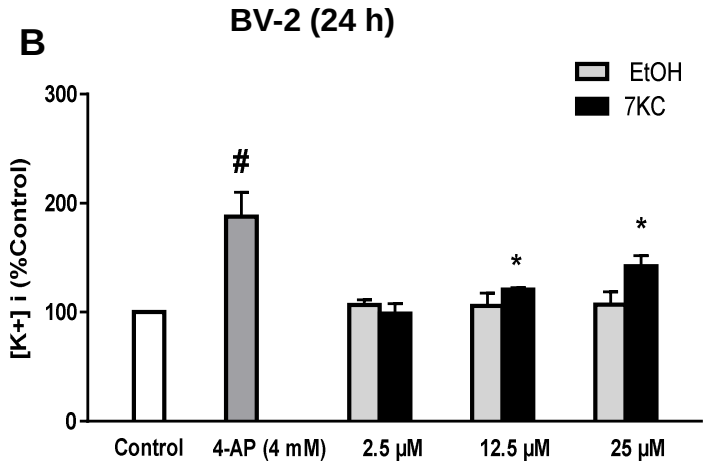

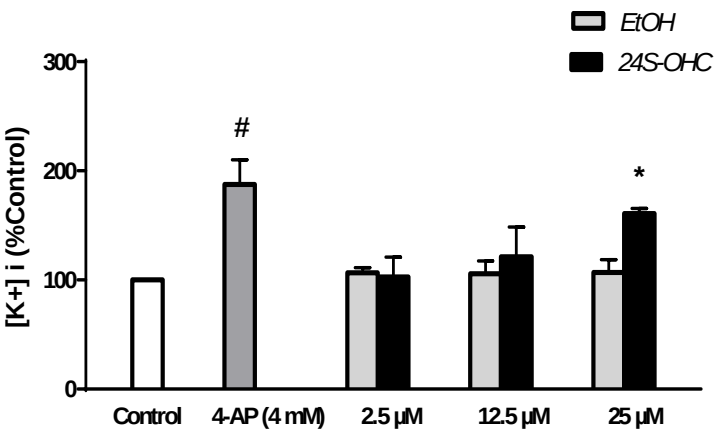

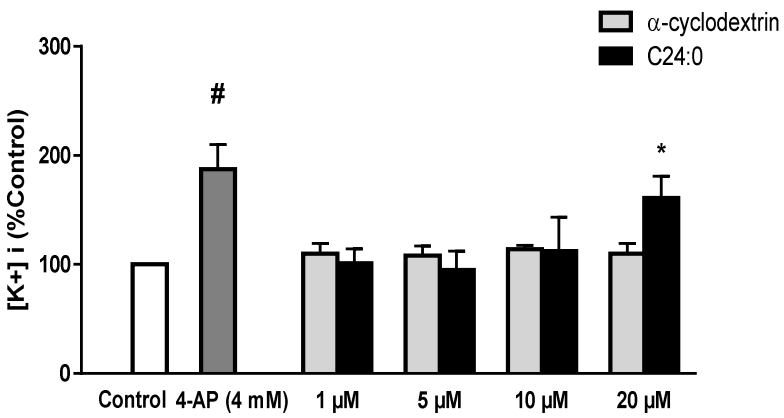

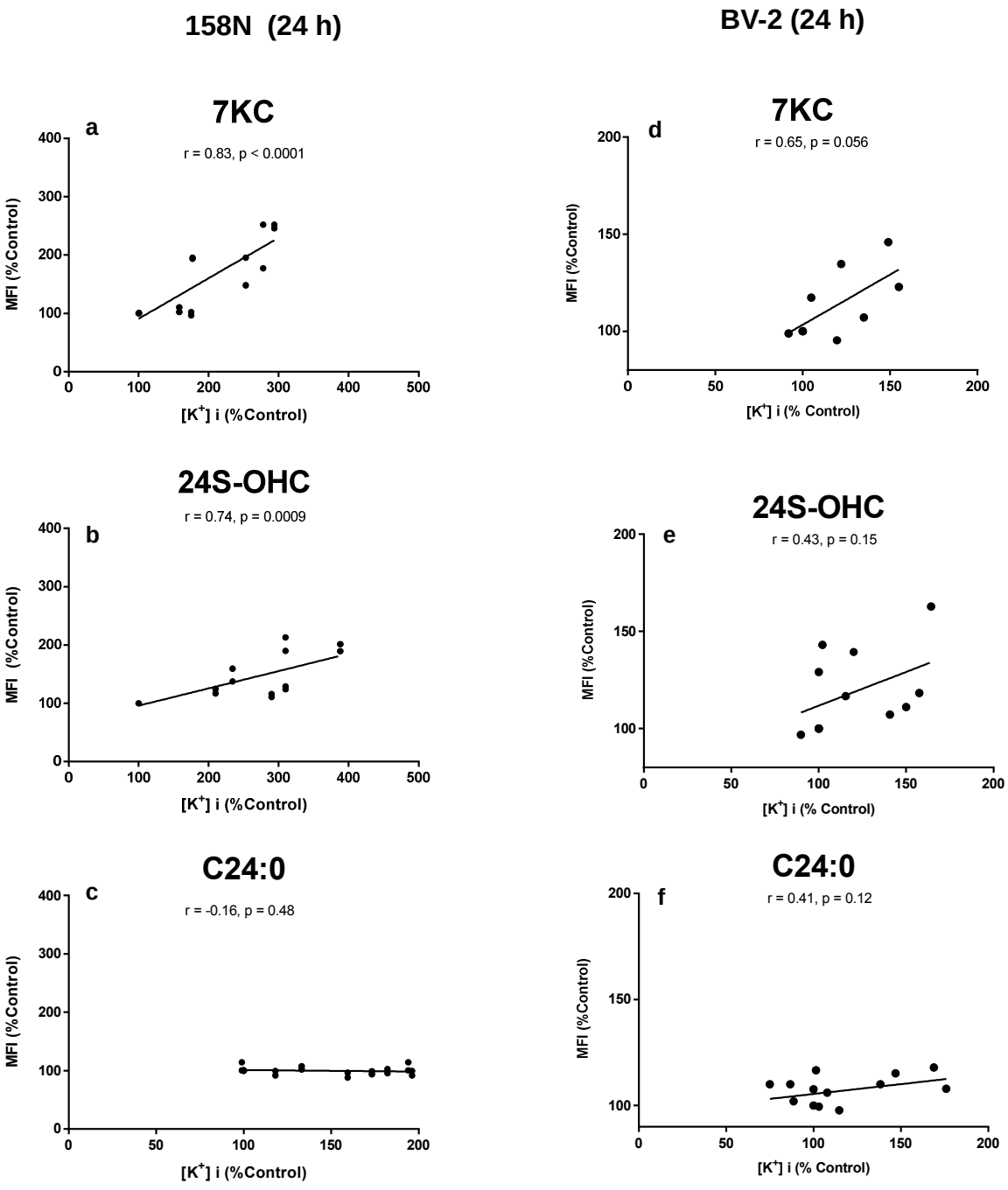

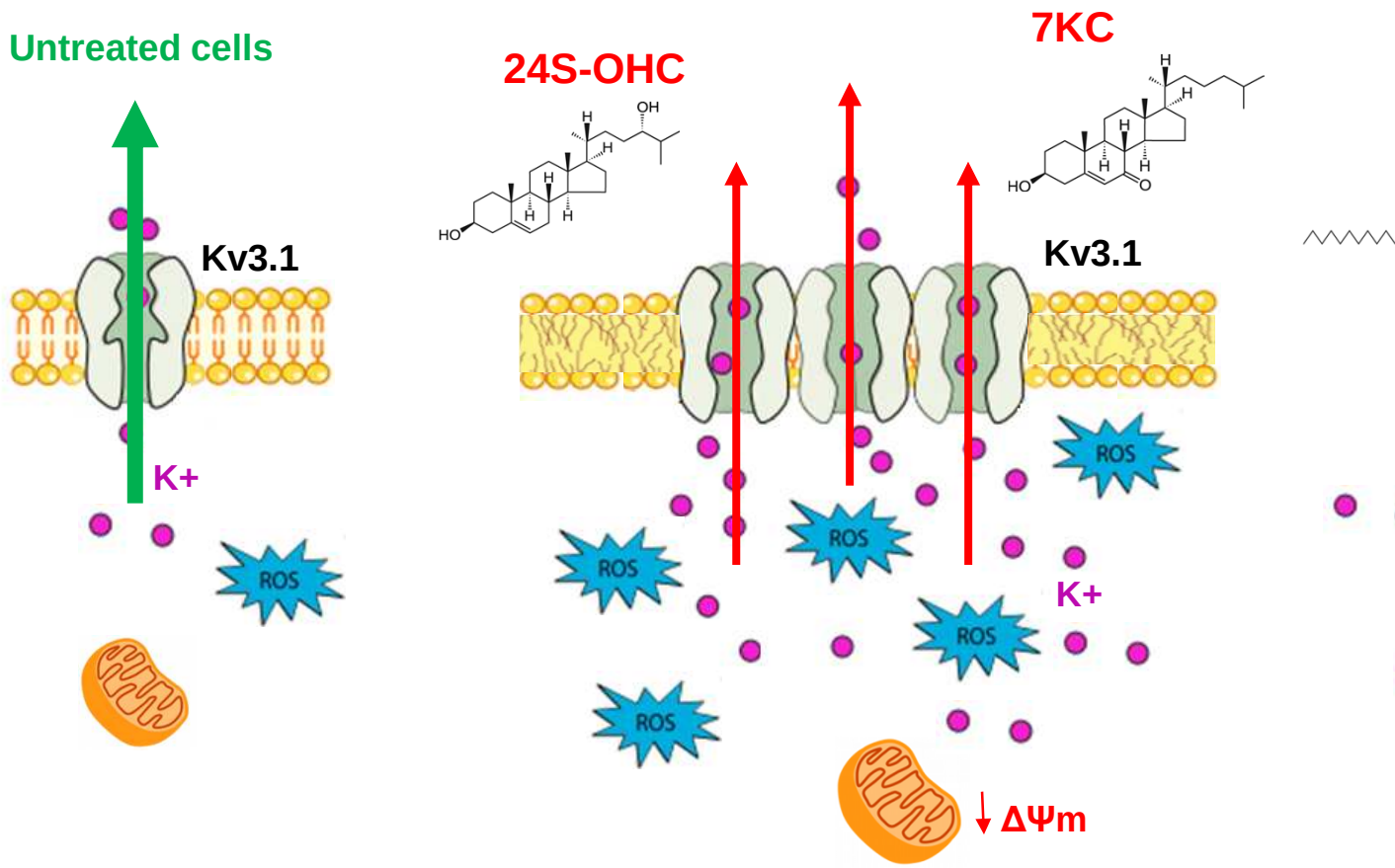

Bezine M et al. , Figure 6

"Modulation of Kv3.1b potassium channel level and intracellular potassium concentration in 158N murine oligodendrocytes and BV-2 murine microglial cells treated with 7-ketocholesterol, 24S-hydroxycholesterol or tetracosanoicacid (C24:0)" by Maryem Bezine *et al.*

- Nerve cells, 158N and BV-2, express Kv3.1b potassium channel
- 7-ketocholesterol, 24S-hydroxycholesterol, and C24:0 modulate Kv3.1b level
- 7-ketocholesterol, 24S-hydroxycholesterol, and C24:0 modulate intracellular K^+ concentration
- Positive correlations between Kv3.1b level, and K^+ accumulation with cell death dysfunctions